Nanoparticles for Targeted Delivery of Therapeutics to Mitochondria to Overcome Drug Resistance

A thesis submitted towards partial fulfillment of

BS-MS Dual Degree Program

by

Syed Muhammed Muazzam Kamil

20111042

under the guidance of

Dr Sudipta Basu

Department of Chemistry

Indian Institute of Science Education and Research, Pune

Certificate

This is to certify that this dissertation entitled "**Nanoparticles for Targeted Delivery of Therapeutics to Mitochondria to Overcome Drug Resistance**" towards the partial fulfilment of the BS-MS dual degree programme at the Indian Institute of Science Education and Research, Pune represents the research carried out by "**Syed Muhammed Muazzam Kamil at Indian Institute of Science Education and Research Pune**" under the supervision of "**Dr Sudipta Basu, Ramalingaswamy Fellow, Department of Chemistry**" during the academic year 2015-2016.

Sudipta Basu

Dr Sudipta Basu

Date: March 28, 2016

Place: IISER Pune

Declaration

I hereby declare that the matter embodied in the report entitled "**Nanoparticles for Targeted Delivery of Therapeutics to Mitochondria to Overcome Drug Resistance**" are the results of the investigations carried out by me at the Department of Chemistry, Indian Institute of Science Education and Research Pune, under the supervision **Dr Sudipta Basu** and the same has not been submitted elsewhere for any other degree.

Syed Muhammed Muazzam Kamil

Date: March 28, 2016

Place: IISER Pune

Acknowledgements

Let me begin by thanking Dr Sudipta Basu for giving me an opportunity to learn and gain valuable research experience in his lab. I have learnt a great deal in the time I have spent in the lab and and have as well grown as an individual. I would like to thank him for his guidance, encouragement and for being patient with me. I would like to express my deep sense of gratitude to him for giving me independence and freedom to learn and work, and for accepting my last minute requests.

It would be unjust if I do not mention my labmates. I would like to thank Abhik who was my mentor when I joined the lab and to this day, has helped me and cleared my doubts. I would also like to thank Sandip and Sohan for their help and suggestions, for clearing my doubts and for discussions (both scientific and non-scientific) during the course of my stay in the lab. I would like to thank Chandramouli for his help whenever needed and to Aditi for bearing me! I would also like to thank Nikunj, Piyush and the new members Shalini, Abhishek and Aman for good times.

Let me also take this opportunity to thank the Director, IISER Pune, Prof. K N Ganesh for providing us the facilities and to thank the faculty, who contributed to my growth. I would like to specially thank Dr Britto Sandanaraj for kindly agreeing to be on my Thesis Advisory Committee and making valuable suggestions.

I am grateful to my friends who were always there with me and taught me valuable lessons.

Last but not least, I would like to thank my family for their constant support, encouragement and belief in me!!

To

my family and teachers

Contents

Figures

Tables

Abstract

Overcoming drug resistance and improving the toxicity profile of drugs are major challenges in cancer chemotherapy. Targeted delivery along with detouring of drugs to cellular organelles and nano-vehicles have emerged as potential solutions to these challenges respectively. In this work, we aimed to deliver electron transport chain (ETC) damaging drug α-tocopheryl succinate and detour nuclear DNA damaging drugs namely cisplatin and camptothecin to mitochondria to overcome the resistance mechanisms against them. We developed sub-200 nm nanoparticles containing these three drugs. The nanoparticles have the zeta potential (ZP) value of 35.1 mV and are stable in phosphate buffer solution (PBS) at 37 ^{o}C and dulbecco's modified eagle medium (DMEM) for 3 days. They were sub-200 nm in size in water at 4 ^{o}C after one month indicating good shelf-life. Their ZP value increased to 40.8 mV in pH 5.5. These nanoparticles are being evaluated for their anti-cancer efficacy and further, their mechanism of action will be studied. We also developed tertiary amine-functionalized nanoparticles based on α-tocopheryl succinate to study the localization of nanoparticles into mitochondria. These nanoparticles are also sub-200 nm in size and have the ZP value > 35 mV. The set of these nanoparticles will be expanded and will be evaluated for mitochondrial localization. Further, we checked the effect of sonication on the size and polydispersity of nanoparticles. We observed that with sonication time, the size decreases with increasing monodispersity.

Introduction

Despite great advances in medicine, cancer remains to be one of the leading causes of deaths in the world. Most of the cancer chemotherapy regimens fail due to the emergence of drug resistance by intrinsic and extrinsic mechanisms.[1] Other concerns include the low concentration of drugs at the target site and off–target side effects.[2] This calls for the discovery of new targets, development of new therapeutics and strategies to accumulate drugs predominantly at the target site to reduce off–target side effects and "intelligent" application of existing drugs.

1.1 Cancer and Nanomedicine

Cancer is the uncontrolled proliferation of cells. It is a consequence of genomic instability, which deregulates the normal functioning of the cell. Cells acquire characteristics like sustaining growth signals, unlimited replicative potential, evading growth suppressors, resistance to cell death, inducing angiogenesis and activating invasion and metastasis. These are the hallmarks of cancer.[3] Recently, two other capabilities – reprogramming energy metabolism and evading immune response are described as the emerging hallmarks of cancer.[4] It is important to note that there is no one-to-one correlation between genetic mutations and the phenotype produced which makes it a very complex disease to understand. A single mutation may lead to two hallmarks and two or more mutations may result in one hallmark.[3]

Cancer is typically treated by surgery, radiation and chemotherapeutics. Chemotherapy is the preferred choice of treatment but it faces challenges like low drug concentration at the pathological site, off-target toxicity, drug resistance and bypass mechanisms in pathological cells. For example, cisplatin is a first line chemotherapeutic drug for solid tumors but it causes neuro- and nephro-toxicities. In cells, its efficacy is reduced by inactivation and efflux among other mechanisms.[5] Doxorubicin is an anticancer drug whose effect is mitigated by repair mechanisms. It also causes cardiotoxicity.[6] To improve the toxicity profile and increase the concentration of drugs at the pathological site, various nanocarriers like micelles, liposomes, vesicles, dendrimers, nanoshells, polymer nanoparticles etc have been developed. These nano-carriers deliver the drug

at the pathological site utilizing the architecture of vasculature at the site of tumors by enhanced permeability and retention (EPR) effect. Thus, decreasing their uptake by other tissues and organs which results in reduced off-target toxicity.[7] This approach of delivering drugs has been successful as the nanoformulations of doxorubicin and paclitaxel are currently on the market and various other formulations are in clinical phase trials.[8] Nanoformulations are being designed to release the drug molecules at the tumor site in response to intrinsic (pH, enzyme concentration etc) and extrinsic (light, magnetic field, electric field) cues.[9] Various nanoformulations based on biocompatible and biodegradable molecules like cholesterol,[10] lithocholic acid[11] and vitamin D3[12] have been developed and evaluated. Nanoformulations are being intelligently designed to release the drug molecules in a slow and sustained manner over a period of time so that the tumor cells succumb to the continuous stress of the drugs.[13,14] Attempts have also been made to enhance the release of drugs from nanoformulations to increase their efficacy.[15] Efforts have been devoted to further increase the specificity of the nanoformulations of the drugs by coating them with the ligands of the over-expressed receptors like folate,[16] biotin[17] etc on the tumor cells. To further increase the therapeutic action of drugs, nanoformulations are being developed to deliver the drug at its target site inside the cell like nucleus[18] and mitochondria.[19,20]

The development of nanoformulations resulted in improved biodistribution of the drugs.[21, 22] This encouraged the development of nanoformulations containing multiple drugs to decrease the effective dose of the drugs. It is demonstrated that three drugs can be delivered using a single nanoformulation and that such a formulation is efficacious as compared to the nanoformulation of two drugs.[23] In this direction, nanoformulations have also been developed to target multiple organelles like nucleus and mitochondria,[24] nucleus and signaling pathways[25,26] etc. Another strategy that is evolving to combat drug resistance is detouring the drugs to other cellular targets. In this area, nuclear DNA damaging drugs are being detoured to mitochondria to damage mitochondrial DNA.[27-30]

In this study, we detour nuclear DNA damaging drugs and deliver mitochondria-acting drug to mitochondria to effect a higher therapeutic outcome.

1.2 Mitochondria

Mitochondria are indispensable for the production of energy in cells and hence for the survival. They also regulate various signaling pathways as many of them converge on mitochondria including that of apoptosis. Thus they also act as suicidal weapon stores of the cell.[31] As a result of its crucial functions in the cell, it has attracted a lot of research interest. Any dysfunction and deregulation of mitochondria would result in diseases. It is linked to cancer, neurodegenerative diseases like Alzheimer's, Parkinson's etc.

A majority of cancer cells have functional mitochondria. It is established that metabolism of mitochondria is required for cancer progression. For the treatment, mitochondrial bioenergetics, biosynthesis production and redox signaling and balance have been targeted.[32] A few studies have also targeted mitochondrial DNA (mtDNA) for therapy. However, the studies that target mitochondria using nanoformulations are very few. Recently, there have been a few reports targeting mitochondria using mesoporous silica,[33] gold nanorods[34] and amphiphilic DNA nanocarriers[35]. Earlier studies demonstrated that the targeted delivery of mitochondria-acting drugs to mitochondria using nanoformulation enhances the efficacy of drugs significantly.[19]

mtDNA and electron transport chain (ETC) are attractive targets for cancer therapy. mtDNA codes for 13 proteins in ETC and their translational machinery.[36] Damaging mtDNA and inhibiting its transcription would result in decreased expression of ETC proteins. This would lead to decreased production of ATP which is against the required demand of growing cancer cells. The cells would succumb to the stress produced. mtDNA can be targeted by detouring nuclear DNA damaging drugs (like cisplatin, doxorubicin, camptothecin etc) to mitochondria and ETC can be targeted by α-tocopheryl succinate. However, detouring nuclear DNA damaging drugs to mitochondria would require mitochondria-directing systems. Delocalized lipophilic cations like triphenylphosphine and mitochondria penetrating peptides (MPPs) are used as mitochondrial transporters. But their homing mechanism into mitochondria is not well understood. However, triphenylphosphine based liposomes[19] and MPP-drug

conjugates[27-29] have been developed to deliver the chemotherapeutics into mitochondria to increase the efficacy and/or to overcome the resistance mechanisms.

This study aims to damage mtDNA with cisplatin and camptothecin and ETC with α-tocopherol succinate.

1.3 Cisplatin

Cisplatin is a chemotherapeutic drug for solid tumors like head, neck etc. It internalizes into the cell by both passive and active mechanisms. It forms DNA-protein and DNA-DNA intrastrand and interstrand crosslinks. However, its cytotoxic action is mainly because of intrastrand crosslinks. Once inside the cell, it loses one of its leaving groups Cl^- and gets aquated. This results in a positively charged species. It then electrostatically moves to the nucleus. In the nucleus, the water molecule is displaced by N7 of guanine. Then, another guanine, either from the same strand or the different, displaces the leaving group Cl^- resulting in intrastrand or interstrand cross links. These crosslinks inhibit its replication and transcription which leads to the activation of apoptotic machinery leading to cell death.[37]

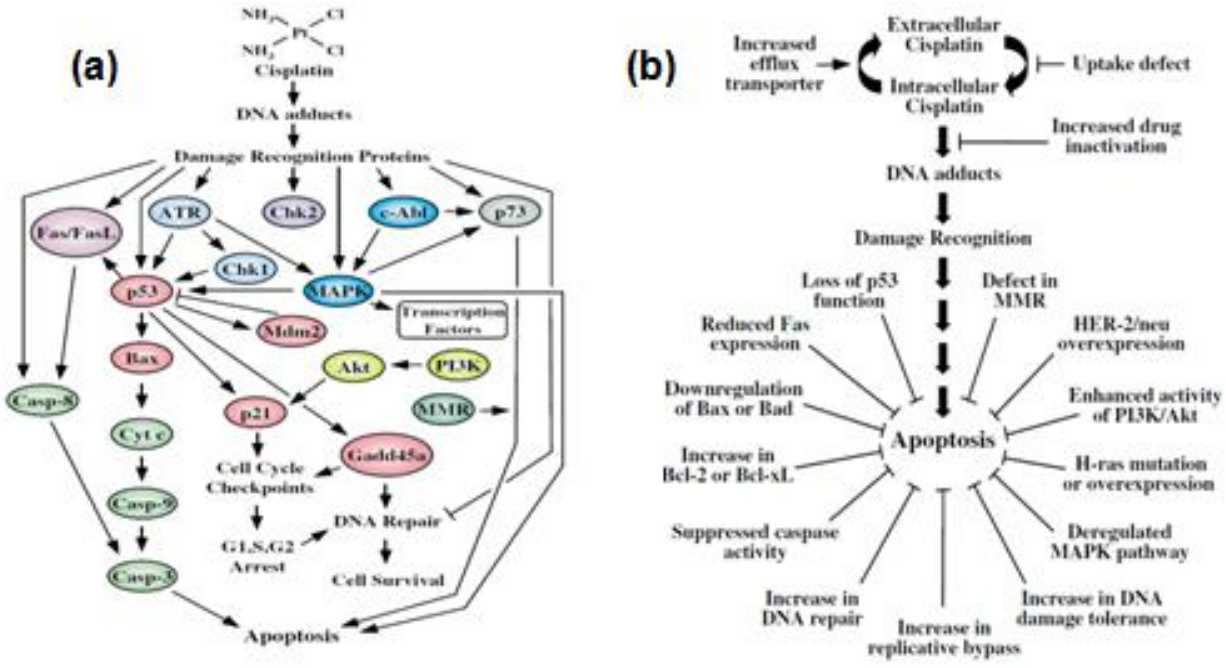

Figure 1: Cellular response (a) to and resistance mechanisms (b) against cisplatin.

As can be seen in the figure (1a) , multiple pathways operate in response to cisplatin to cause cell death. But, cancer cells develop multiple resistance mechanisms to negate the cytotoxic action which are as complex as the cellular response as can be seen in the figure (1b). This drug also causes nephrotoxicity.[5]

Various nanoformulations have been developed of cisplatin to reduce its toxicity and enhance efficacy. A nanoparticle has been developed to enhance its efficacy based on structure-activity relationships.[38] It has also been used in combination with other drugs to enhance its efficacy.[24-26] A hyaluronic acid based nanoconjugate has been developed to reduce toxicity and improve survival.[39] However, mtDNA would be a new target for cisplatin. Thus, it can overcome the resistance mechanisms that the cells have developed when it forms adducts with nuclear DNA.

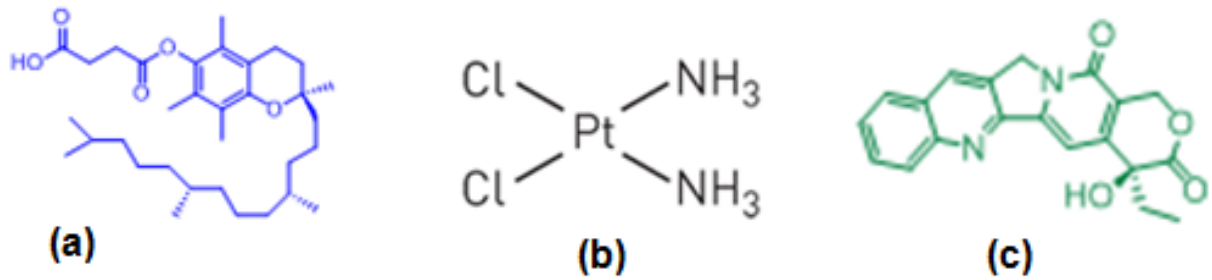

Figure 2: Structures of α-tocopheryl succinate (a), cisplatin (b) and camptothecin (c).

1.4 Camptothecin

It is a DNA Topoisomerase 1 (topo1) inhibitor. topo1 reversibly relaxes the superhelical tension that the DNA undergoes while replication, transcription and recombination. It stabilizes the topo 1 and DNA complex. This results in apoptosis. It is interesting to note that it does not interact with topo1 or DNA alone but only with their binary complex. However, it is hydrophobic and therefore less soluble in blood. It causes neurotoxicity. Also, cells over time develop resistance mechanisms against it like low cellular accumulation, efflux and change in response to the complex formation with topo1-DNA complex. Additionally, certain mutations may occur which may result in resistance against camptothecin.[40] To overcome the solubility issue, it has been conjugated to cyclodextrin.[41] The conjugate shows improved efficacy when compared with the free

drug. It has also been realized in combination therapy with curcumin[42] and doxorubicin.[43] If this drug is detoured to mitochondria, it would overcome the resistance mechanisms like cellular response to the complex of topo1-DNA as this would be new to the mitochondrial machinery. Sequestering the drug into mitochondria would also decrease the efflux of the drug which results in higher cellular concentration. This may yield higher therapeutic outcome.

1.5 α-Tocopheryl Succinate

It is a succinate derivative of vitamin E. It inhibits complex II of ETC in mitochondria which results in enhanced production of Reactive Oxygen Species (ROS). The increased amount of ROS generated damages DNA and proteins and leads to cell death.[44] It stops cell proliferation at low concentrations and causes cell death at higher concentrations. In general, it effects therapeutic action at higher concentrations. To increase its efficacy, it was delivered to mitochondria encapsulated in positively charged polymeric nanoparticles.[19] This approach enhanced its efficacy significantly. It's acid functional group is a good handle to conjugate it to other drugs. This has been explored by the researchers to conjugate it to nuclear DNA damaging drugs like cisplatin and doxorubicin.[24] It was also conjugated to mitochondria-targeting molecule and subsequently engineered into a nanoparticle encapsulating an anti-apoptotic protein (BCL-2) inhibitor obatoclax.[20] However, the most remarkable aspect of this molecule is that it is non-toxic to non-cancerous cells.

We aim to develop a mitochondria-targeting nanoplatform based on α-tocopheryl succinate encapsulating nuclear DNA damaging drugs to deploy them in mitochondria to damage mitochondrial DNA. This nanoplatform would also disrupt the function of ETC by inhibiting complex II. We anticipate that such a nanoplatform would be very effective as the design encompasses the strategy to overcome drug resistance and also to deliver the drugs in higher amounts at the site of their targets.

Materials and Methods

2.1 Materials and Instruments

The chemicals and dry solvents were purchased Sigma-Aldrich Chemicals and Avanti Polar Lipids. NMR spectra were recorded on 400 MHz Jeol spectrometer. The size, polydispersity and zeta potential were measured by dynamic light scattering (DLS) on Nano ZS-90 apparatus. It is equipped with 633 nm laser supplied by Malvern instruments. The absorption studies were done using Perkin-Elmar Lambda 45 spectrometer.

2.2 Procedures

2.2.1 Synthesis of triphenylphosphine-functionalized α-tocopheryl succinate (scheme 1)

Synthesis of α-tocopheryl succinate and 5-bromopentanol conjugate (3)

α-tocopheryl succinate (**1**) (200 mg, 0.3768 mmol, 1 equiv) was dissolved in 5 mL dry dichloromethane (DCM) under nitrogen atmosphere in a two-neck round-bottom flask. To the solution was added N,N'-dicyclohexylcarbodiimide (DCC) (93 mg, 0.4524 mmol, 1.2 equiv) and dimethylaminopyridine (DMAP) (22.4 mg, 0.1884 mmol, 0.5 equiv). The solution was stirred for half an hour in an ice bath. Into the solution was then added 5-bromopentanol (91.26 µL, 0.7536 mmol, 2 equiv). The mixture was stirred at 25 ^{o}C and the reaction was monitored by thin layer chromatography (TLC). After 3 h, the reaction mixture was diluted to 30 mL by adding DCM and filtered using whatmann filter paper to separate the urea formed in the reaction. The organic layer was concentrated under vacuum. The product (**3**) was purified using silica gel (100-200 mesh size) column chromatography in EtOAc:pet ether mobile phase. The product eluted at EtOAc:pet ether = 1:24. The yield was 51 %.

Synthesis of triphenylphosphine-functionalized α-tocopheryl succinate (4)

α-tocopheryl succinate and 5-bromopentanol conjugate (**3**) (60 mg, 0.0883 mmol, 1 equiv) was dissolved in 5 mL dry acetonitrile (ACN) under inert atmosphere in a two-

neck round-bottom flask. Into the solution were added triphenylphosphine (46.32 mg, 0.1766 mmol, 2 equiv) and 35 mg of potassium carbonate (K_2CO_3). The solution was refluxed at 85 ^oC for 24 h. After 24 h, potassium carbonate was removed from the reaction mixture by decanting the acetonitrile solution into another flask. The solution was then concentrated under vacuum. The product was purified using silica gel (100-200 mesh size) column chromatography in MeOH:DCM mobile phase. The product eluted at MeOH:DCM = 1:19. The yield was 34 %.

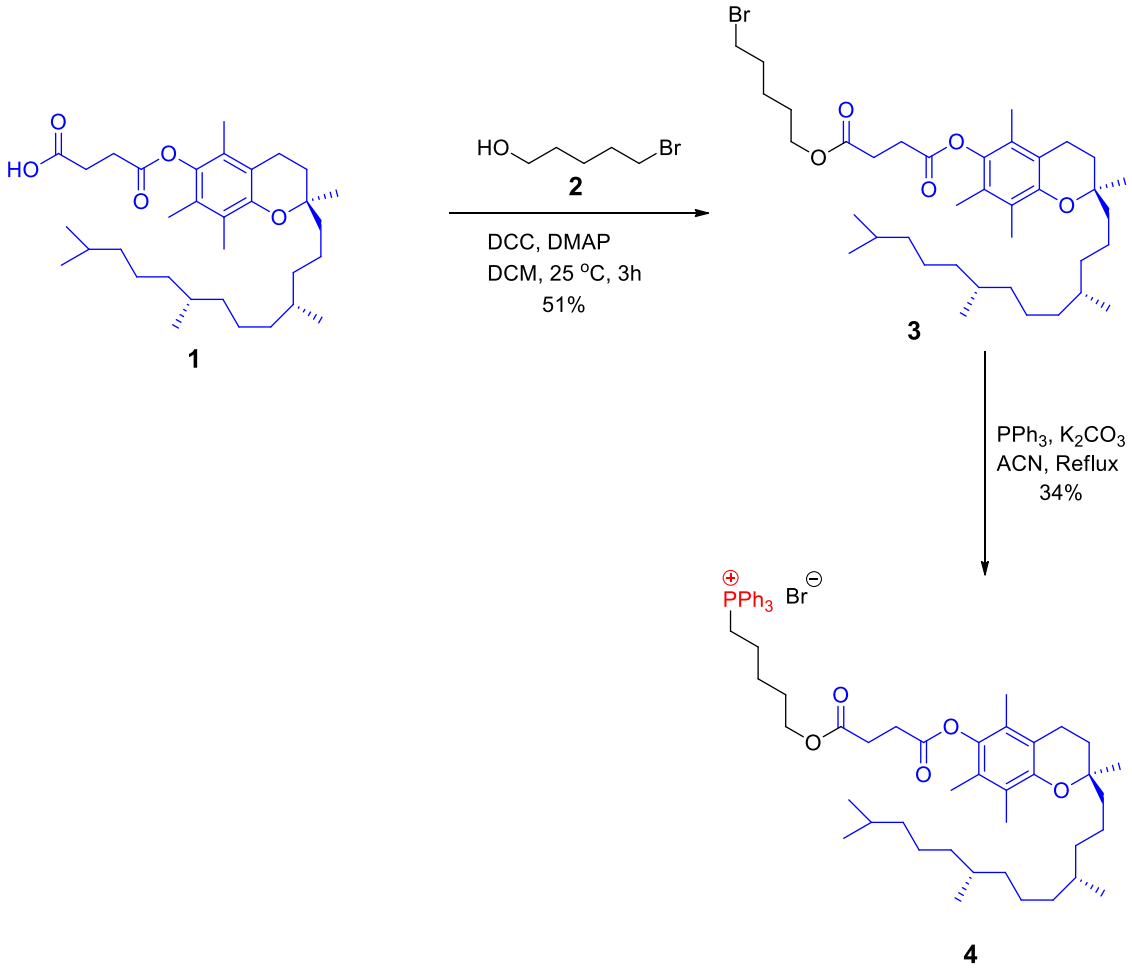

Scheme 1: Synthesis of triphenylphosphine-functionalized α-tocopheryl succinate.

2.2.2 Synthesis of α-tocopheryl succinate -cisplatin conjugate (scheme 2)

Synthesis of aquated cisplatin (6)

Cisplatin (**5**) (50 mg, 0.1666 mmol, 1 equiv) was dissolved in 10 mL distilled water in a vial. To the solution was added silver nitrate (28 mg, 0.1666 mmol, 1 equiv). The solution was stirred at 25 ^{o}C for 24 h in dark. It was observed that the solution turned milky. After that, the solution was thrice centrifuged for 15 min at 7000 rpm. The supernatant aquated cisplatin (**6**) was collected and stored in dark.

Synthesis of α-tocopheryl succinate-cisplatin conjugate (7)

α-tocopheryl succinate (**1**) (5 mg, 0.0094 mmol, 1 equiv) was dissolved in 1 mL dry dimethyl formamide (DMF) in a clean vial. Aquated cisplatin (**6**) (2.5 mg, 0.0094 mmol, 1 equiv) was added to the solution slowly. The solution was stirred for 24 h at 25 ^{o}C in dark. After that, the solvent was evaporated under vacuum to collect the product (**7**). The yield was 89 %. The product was stored in dark.

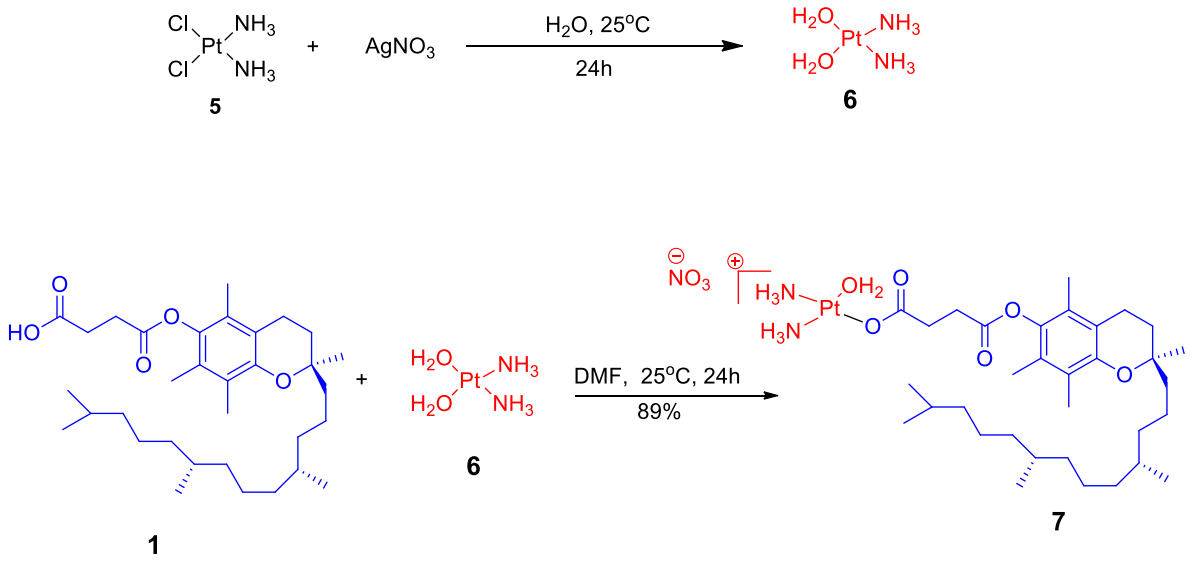

Scheme 2: Synthesis of α-tocopheryl succinate-cisplatin conjugate.

2.2.3 Synthesis of tertiary amine-functionalized α-tocopheryl succinate (scheme 3)

Synthesis of pyridine-functionalized α-tocopheryl succinate (8)

α-tocopheryl succinate and 5-bromopentanol conjugate (**3**) (50 mg, 0.0735 mmol) was dissolved in 3 mL dry pyridine (Py) under nitrogen atmosphere in a clean two-neck round-bottom flask. The solution was refluxed at 80 ^{o}C for 48 h. After that, pyridine was evaporated under vacuum. The product (**8**) was purified using silica gel (100-200 mesh size) column chromatography in MeOH:DCM mobile phase. The product eluted at MeOH:DCM = 1:16. The yield was 85 %. In this reaction, pyridine was used both as a solvent and a reactant.

Synthesis of dimethylaminopyridine-functionalized α-tocopheryl succinate (9)

α-tocopheryl succinate and 5-bromopentanol conjugate (**3**) (60 mg, 0.0883 mmol) was dissolved in 3 mL dry toluene under inert atmosphere in a clean two-neck round-bottom flask. To the solution was added dimethylaminopyridine (20.35 mg, 0.1666 mmol, 2 equiv). The solution was refluxed at 80 ^{o}C for 48 h. After that, the solvent was evaporated under vacuum. The product (**9**) was purified using silica gel (100-200 mesh size) column chromatography in MeOH:DCM mobile phase. The product eluted at MeOH:DCM = 1:16. The yield was 89 %.

Synthesis of triethylamine-functionalized α-tocopheryl succinate (10)

α-tocopheryl succinate and 5-bromopentanol conjugate (**3**) (50 mg, 0.0735 mmol) was dissolved in 3 mL dry triethylamine (TEA) under inert conditions in a clean two-neck round-bottom flask. The solution was refluxed at 80 ^{o}C for 48 h. After that, the solvent was evaporated under vacuum. The product (**10**) was purified using silica gel (100-200 esh size) column chromatography in MeOH:DCM mobile phase. The product eluted in MeOH:DCM = 1:24. The yield was 63 %. In this reaction, triethylamine was used both as a reactant and solvent.

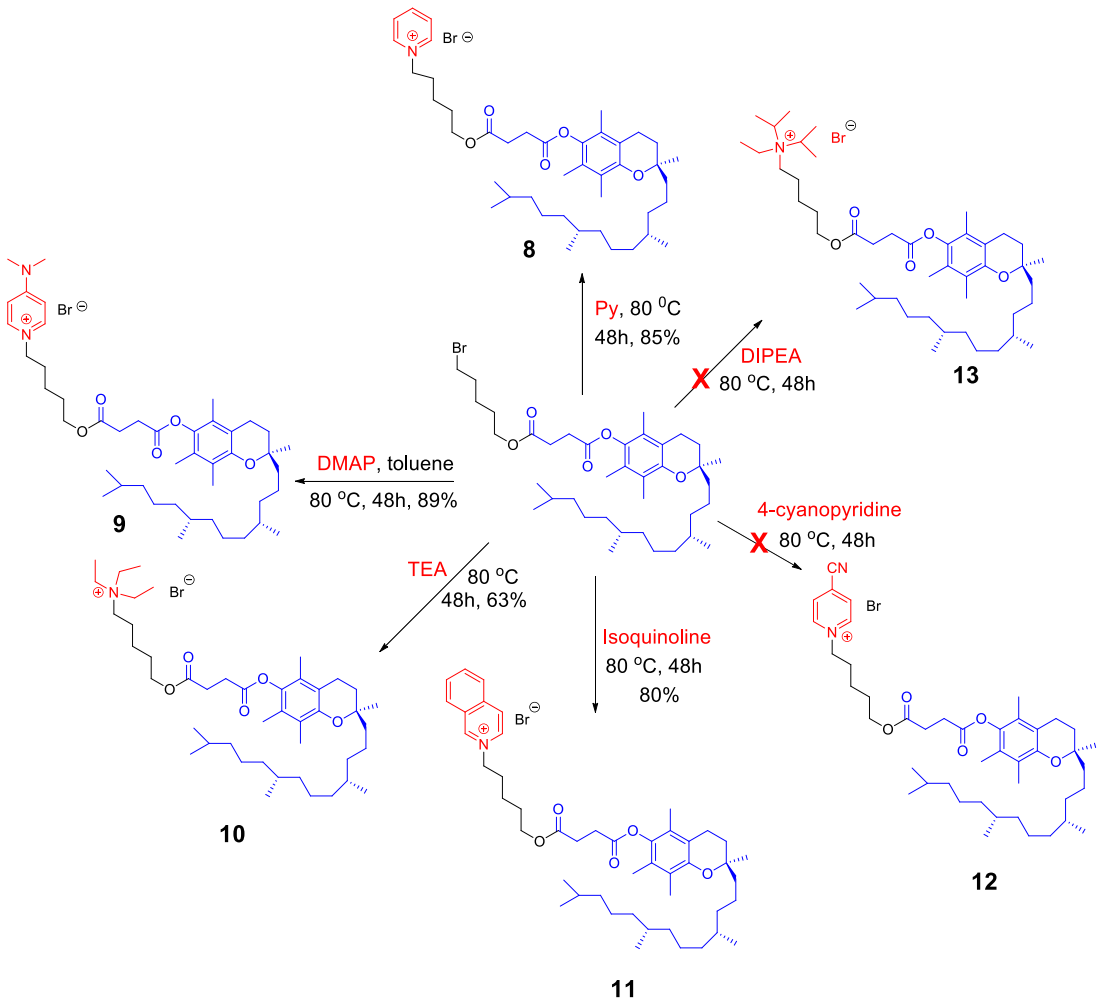

Scheme 3: Synthesis of tertiary amine-functionalized α-tocopheryl succinate.

Synthesis of isoquinoline-functionalized α-tocopheryl succinate (11)

α-tocopheryl succinate and 5-bromopentanol conjugate (**3**) (40 mg, 0.0588 mmol) was dissolved in 3 mL isoquinoline under inert conditions in a clean two-neck round-bottom flask. The solution was stirred at 80 ºC for 48 h. After 48 h, the product (**11**) was purified using silica gel (100-200 mesh size) column chromatography in MeOH:DCM mobile phase. The solvent could not be evaporated after stopping the reaction because of high boiling point of isoquinoline (> 242 ºC). So, the reaction mixture was used as such for column chromatography purification. The product eluted in MeOH:DCM = 1:49. The yield was 80 %. In this reaction, isoquinoline was used both as a reactant and solvent.

Attempted synthesis 4-cyanopyridine-functionalized α-tocopheryl succinate (12)

α-tocopheryl succinate and 5-bromopentanol conjugate (**3**) (13.4 mg, 0.0197 mmol, 1 equiv) was dissolved in 2 mL toluene under nitrogen atmosphere in a clean two-neck round-bottom flask. To the solution was added 4-cyanopyridine (5.2 mg, 0.05 mmol, 2.5 equiv). The solution was refluxed at 80 ^{o}C for 48 h. However, the reaction did not yield the expected product (**12**).

Attempted synthesis of diisopropylethylamine-functionalized α-tocopheryl succinate (13)

α-tocopheryl succinate and 5-bromopentanol conjugate (**3**) (10 mg, 0.0147 mmol) was dissolved in 2 mL diisopropylethylamine (DIPEA) under nitrogen atmosphere in a clean two-neck round-bottom flask. The solution was refluxed at 80 ^{o}C for 48 h. However, the reaction did not yield the expected product (**13**). In this reaction, DIPEA was used as the reactant as well as the solvent.

2.2.4 Synthesis of vitamin D3-cisplatin conjugate (scheme 4)

Synthesis of vitamin D3-succinic anhydride conjugate (15)

Vitamin D3 (**14**) (100 mg, 0.2599 mmol, 1 equiv) was dissolved in 4 mL dry DCM under inert atmosphere in a clean two-neck round-bottom flask. To the solution was added 1.5 mL dry pyridine. The solution was cooled to 0 ^{o}C. Then succinic anhydride (260 mg, 2.6 mmol, 10 equiv) and dimethylaminopyridine (15.8mg, 0.129 mmol, 0.5 equiv) were added. The solution was stirred at 25 ^{o}C for 24 h. After 24 h, the reaction was quenched by adding a few drops of 1N HCl. The pH of the quenched reaction mixture was 6-7. To the reaction mixture was then added 30 mL DCM. The organic layer was washed with brine (3 x 30 mL). It was then dried over Na_2SO_4. The product (**15**) was purified using silica gel (100-200 mesh size) column chromatography in EtOAc:pet ether mobile phase. The product eluted in EtOAc:pet ether = 1:6. The yield was 32.2 %.

Synthesis of vitamin D3-cisplatin conjugate (16)

Vitamin D3-succinic anydride conjugate (**15**) (25 mg, 0.0515 mmol, 1 equiv) was dissolved in 2 mL DMF in a clean vial. To the solution was added aquated cisplatin (**6**) (2.866 mL, 0.0515 mmol, 1 equiv). The solution was stirred at 25 ^{o}C for 24 h. After that, the solvent was evaporated to collect the product (**16**). The yield was 85 %.

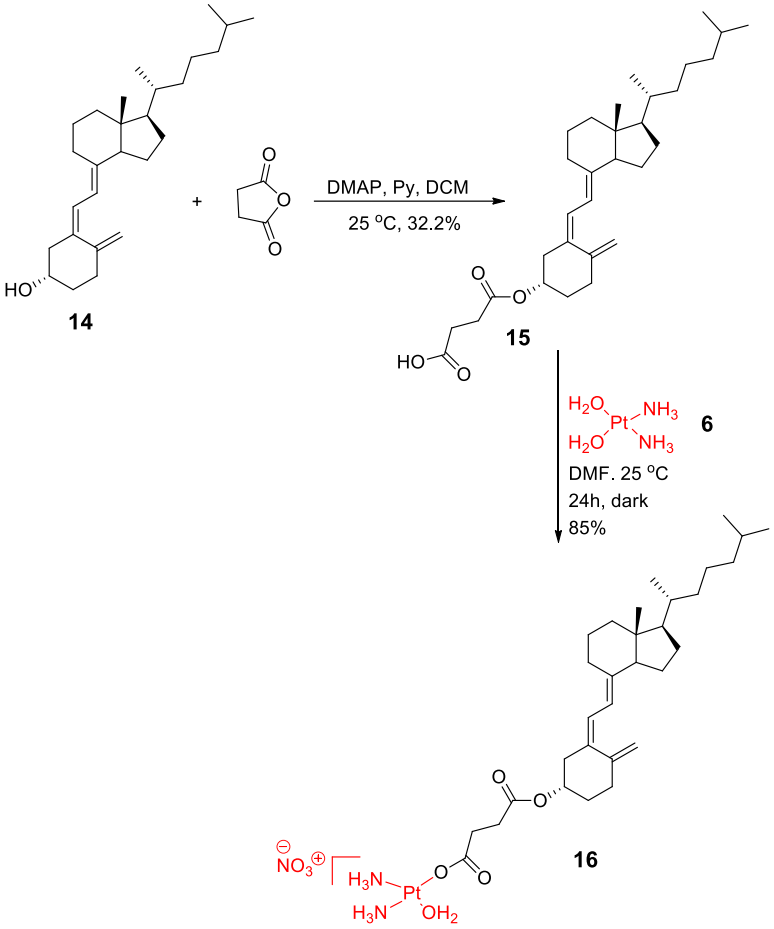

Scheme 4: Synthesis of viramin D3-cisplatin conjugate.

2.2.5 Synthesis of triphenylphosphine-functionalized vitamin D3 (18) (scheme 5)

(4-carboxybutyl)triphenylphosphonium bromide (**17**) (50 mg, 0.1127 mmol, 1 equiv) was dissolved in 10 mL of dry DCM under inert atmosphere in a clean two-neck round-bottom flask. To the solution were added 1-ethyl-3-(3-dimethylaminopropyl)carbodiimide (EDCI) (43.20 mg, 0.2254 mmol, 2 equiv) and dimethylaminopyridine (13.76 mg, 0.1127

mmol, 1 equiv). The solution was stirred in an ice bath for half an hour. After that, vitamin D3 (**14**) (65.02 mg, 0.1690 mmol, 1.5 equiv) was added. The reaction mixture was then stirred for 24 h at 25 ^{o}C. After that, the reaction mixture was diluted by adding 20 mL of DCM. The pH was then neutralized by adding a few drops of 1N HCl. The organic layer was washed with brine (3 x 30 mL) and dried over Na_2SO_4. The organic layer was then concentrated in vacuum. The product (**18**) was purified by using column chromatography in MeOH:DCM mobile phase. The product eluted in MeOH:DCM = 1:32. The yield was 31 %.

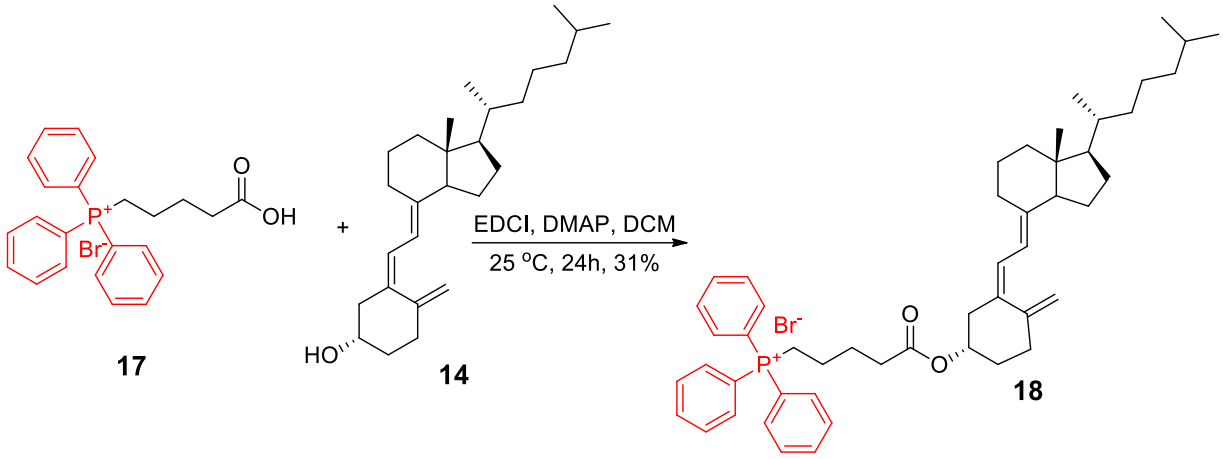

Scheme 5: Synthesis of triphenylphosphine-functionalized vitamin D3.

2.2.6 Attempted Synthesis of camptothecin conjugated molecules (scheme 6)

α-tocopheryl succinate (**1**) (10 mg, 0.0188 mmol, 1 equiv) was dissolved in 3 mL of dry DCM under inert atmosphere in a clean two-neck round-bottom flask. To the solution were added EDCI (7.2 mg, 0.0376 mmol, 2 equiv) and DMAP (2.3 mg, 0.0188 mmol, 1 equiv). The solution was stirred for half an hour in an ice bath. After that, camptothecin (**19**) (7.2 mg, 0.0206 mmol, 1.1 equiv) was added to the solution. The solution was then stirred for 24 h at 25 ^{o}C. After 24 h, the reaction mixture was diluted to 30 mL by adding DCM. Organic layer was then washed with brine (3 x 30 mL). MALDI-TOF spectrometry of the organic layer showed the mass of the desired product (**20**). However, after purification using column chromatography in EtOAc:pet ether mobile phase, the desired

product was not confirmed by NMR spectroscopy. The reaction with vitamin D3-succinic anhydride conjugate (**15**) also did not give the desired product. As in this case, MALDI-TOF spectrometry showed the mass of the desired product.

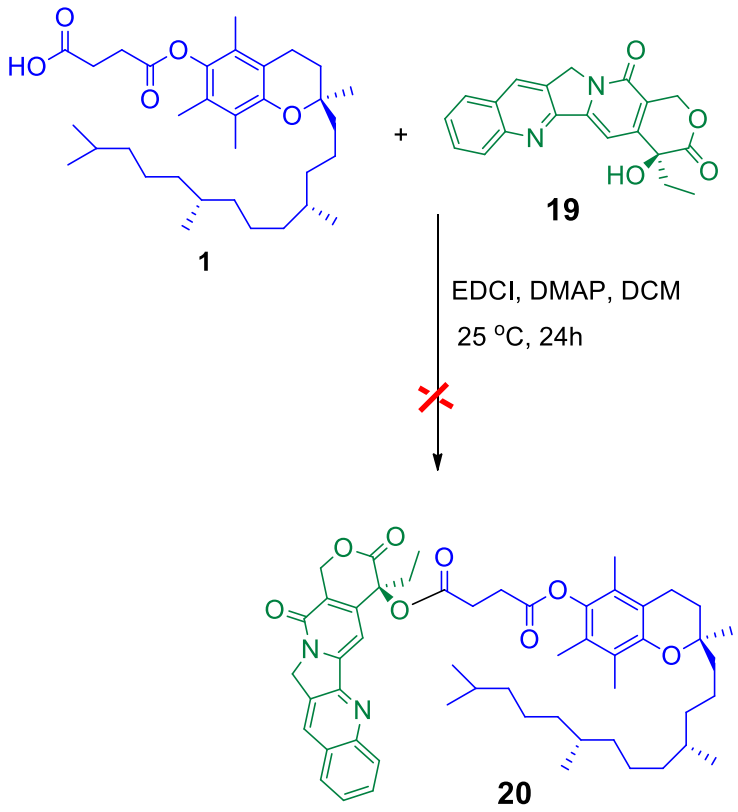

Scheme 6: Synthesis of α-tocopheryl succinate-camptothecin conjugate.

2.2.7 Standard calibration curve of camptothecin by UV-Vis spectroscopy

A standard curve of camptothecin was plotted in the concentration range 5 µM to 30 µM in dimethyl sulfoxide (DMSO). The concentrations were prepared by diluting 1 mM stock solution of camptothecin in DMSO and the absorbance was measured at 367 nm (which is a characteristic wavelength of camptothecin). The linear fit for absorbance against concentration was $y = 0.0199x$ with $R^2 = 0.9954$.

Conc. (µM)	5	10	15	20	25	30
Absorbance	0.1	0.176	0.285	0.394	0.505	0.606

Table 1: Absorbance of camptothecin at 367 nm in various concentrations.

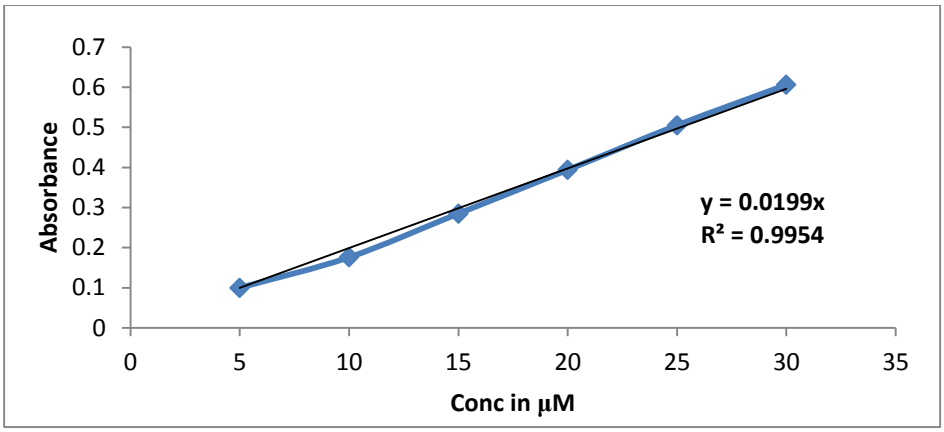

Figure 3: Standard curve of camptothecin by UV-Vis spectrometry

The standard curves of cisplatin and α-tocopheryl succinate were available in the lab and were used as such. The characteristic wavelength for cisplatin and α-tocopheryl succinate are 706 nm and 288 nm respectively and their respective linear fits are y = 0.0355x and y = 0.0016x.

2.2.8 Synthesis of nanoparticles (NPs) and their characterization

Synthesis of triphenylphosphine-functionalized nanoparticles containing camptothecin and/or cisplatin

The nanoparticles were synthesized with varying content of triphenylphosphine-functionalized α-tocopheryl succinate (**4**), α-tocopheryl succinate-cisplatin conjugate (**7**) and camptothecin (**19**). The amount of L-α-phosphatidyl choline (PC) taken was twice and of 1,2-distearoyl–sn-phosphoethanolamine-N-[amino(polyethylene glycol)-2000] (DSPE-PEG_{2000}) was one-tenth the amount of above three components. All the components were dissolved in DCM. It was then slowly evaporated using rotary evaporator to give a lipid-film. The lipid film was dried under vacuum for 15 minutes and then hydrated with 1 mL of distilled water for 2 hr at 60 ^{o}C. After hydration, the solution was passed through Sephadex G-25 and the turbid solution was collected. The collected solution was then extruded through a 200 nm filter. In total, 5 NPs were synthesized with varying content of the three components (**4**, **7**, **19**). The nanoparticles were then characterized. Following table lists the NPs synthesized.

NP	Compound 4	Compound 7	Compound 19	PC	DSPE-PEG
	(mg)	(mg)	(mg)	(mg)	(mg)
NP1	1	0.5	1	5	0.25
NP2	0.5	1	1	5	0.25
NP3	1	1	1	6	0.3
NP4	1	0	1	4	0.2
NP5	1	1	0	4	0.2

Table 2: Nanoparticles synthesized and their compositions.

Synthesis of tertiary amine-functionalized nanoparticles

Nanoparticles were synthesized for compounds 8, 9 and 11 by taking 1 mg of the compound, 2 mg of PC and 0.1 mg of DSPE-PEG_{2000}. The protocol above was followed for the synthesis. The nanoparticles synthesized were NP6, NP7 and NP8 respectively.

Determination of size and charge of nanoparticles

For the determination of size, 50 μL on nanoparticle solution was dissolved in 950 μL of distilled water. The size of the nanoparticles and polydispersity were determined using dynamic light scattering (DLS). The charge of the nanoparticles was determined by measuring zeta potential (ZP) on the same instrument.

Determination of drug content in the nanoparticles

For the determination of camptothecin and α-tocopheryl succinate, three nanoparticle solutions of different dilutions were prepared in spectroscopy grade DMSO. The dilutions were 10, 15 and 20. For the determination of cisplatin, three nanoparticle solutions of different dilutions were prepared in spectroscopy grade DMF solution of o-phenylenediamine (1.2 mg of o-phenylenediamine in 1 mL of DMF). The dilutions were 20, 30 and 40. The solutions were heated at 90 ^{o}C for 2 hr. The absorbance was measured at their characteristic wavelengths against the corresponding blank solutions.

Stability of nanoparticles

Stability of nanoparticles was determined in water at 4 ^{o}C, phosphate buffer solution (PBS) at 37 ^{o}C and dulbecco's modified eagle medium (DMEM) at 37 ^{o}C by measuring

their size and polydispersity using DLS. The measurements were taken at pre-determined time points.

2.3 Instrumentation

Field-Emission Scanning Electron Microscopy (FESEM)

The nanoparticle solution was diluted 15 times. From the diluted solution, 5 µL was drop casted onto silicon wafer and it was dried under vacuum. The sample was then analysed and images were taken using Ultra-55, Zeiss NTS GmbH operating at 4.0 KV.

Results and Discussions

In order to study organelle chemical biology or to effect the higher therapeutic outcome of the drugs targeting various organelles, the probes or the drugs should be specifically delivered to the organelle.[45] Usually, once the probes/drugs enter the cell, they diffuse and meet their target. Many of them lose their function because of unspecific and undesired interactions with cellular milieu.[19] Essentially only few molecules reach their site of action. As far as drug molecules are concerned, this decreases their efficacy significantly and results in medication for longer times which may result in side effects. To address the concern of delivery of drugs to the organelle, we are functionalizing.the drug with the organelle targeting molecule. This approach is being used to deliver the drugs to the organelle of choice as shown in a few reports. [19,20, 27-31]

α-tocopheryl succinate targets ETC in mitochondria but it effects therapeutic outcome at higher concentrations. To increase its concentration in mitochondria, we have functionalized it with triphenylphosphine. α-tocopheryl succinate was conjugated to 5-bromopentanol via an esterification reaction. The bromine in the conjugate (**3**) was then replaced by triphenylphosphine to afford a positively charged molecule (**4**). This molecule would home into mitochondria because of a very high negative inner membrane potential (~ 150 mV) of mitochondria.[31] Motivated by the study that compound (**4**) can be engineered into a nanoparticle which can encapsulate drug molecules and homes into mitochondria,[20] we sought to engineer a nanoparticle containing DNA damaging drugs to damage mitochondrial DNA. Such a detouring of nuclear DNA damaging drugs to mitochondria would overcome the resistance mechanism that the cells have developed against them. We chose the DNA damaging drugs cisplatin and camptothecin. Cisplatin was conjugated to α-tocopheryl succinate (**7**). However, α- tocopheryl succinate and camptothecin conjugate (**20**) was not confirmed by NMR spectroscopy. So, we proceeded to synthesize nanoparticles with compounds (**4**), (**7**) and (**19**) as described in procedures section.

We also synthesized triphenylphosphine-functionalized vitamin D3 (**18**) and vitamin D3-cisplatin conjugate (**16**). These molecules would be used to synthesize cisplatin and

camptothecin based control nanoparticles containing one drug and two drugs and thus check their efficacy against the α-tocopheryl succinate based three drug containing nanoparticles. As with α-tocopheryl succinate, we could not get vitamin D3-camptothecin conjugate.

3.1 Studies on the triphenylphosphine-functionalized nanoparticles

3.1.1 Characterization of nanoparticles

The size, polydispersity and zeta potential (ZP) of NPs were determined by DLS. The data is shown below in table (3).

	NP1	NP2	NP3	NP4	NP5
Size (nm)	432.4 ± 14.5	283.5 ± 13.7	112.7 ± 2.7	148 ± 3.1	145.2 ± 1.9
PDI	0.67 ± 0.01	0.37± 0.03	0.07 ± 0.02	0.22 ± 0.04	0.17 ± 0.00
ZP (mV)	38.6 ± 1.6	32.7 ± 1.3	35.1 ± 2.1	24 ± 3.0	24 ± 2.9

Table 3: Size, PDI and ZP of triphenylphosphine-functionalized nanoparticles.

As can be seen, the average size of the NP1 and NP2 are 432.4 nm and 283.5 nm respectively. The size distribution of NP1 and NP2 can be seen in the figure (4a, 4b) Since the nanoparticle solution was extruded through 200 nm filter, the > 200 nm size of nanoparticles suggests aggregation. Such a size is not desirable for biological applications as they are cleared by reticuloendothelial sytem. The desirable size range is 10 nm – 200 nm.[7] The NPs NP1 and NP2 were not studied further. The size of other NPs are in the desirable range for biological applications and they are also monodisperse as suggested by low PDI values. NP3 is the most monodisperse with the average PDI value of 0.07. NP3 contains three drugs whereas NP4 and NP5 are two drug controls. Thus, we optimized size, PDI and surface charge for three drugs containing nanoparticles by varying the composition of three components (**4**, **7**, **19**). The optimized NP3 was further studied. The size distribution of NP4 and NP5 can be seen in figure (4c, 4d) and of NP3 in figure (5a).

The NP3 was spherical in shape as can be seen in FESEM image (figure 6). The size of NP observed in FESEM image was in accordance with that determined by using DLS. To be successful in clinics, the NP should be stable at 4 ^{o}C and 37 ^{o}C. Moreover, NPs

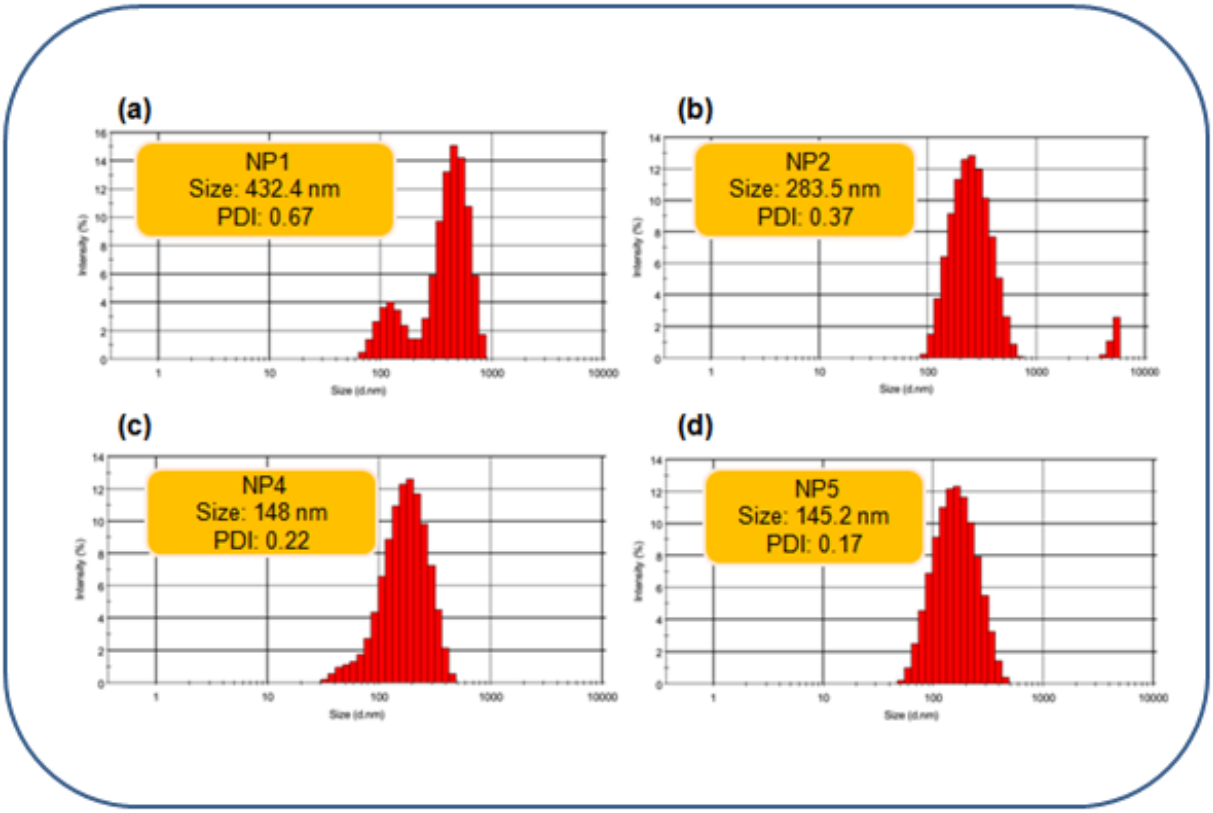

Figure 4: Size distribution of NP1, NP2, NP4 and NP5. Average size and PDI are shown in the box.

should be stable in blood circulation for extended period for accumulating into tumor by EPR effect. NP3 met these requirements. It was stable in PBS at 37 ^{o}C and DMEM. The stability was checked for 3 days in PBS as it mimicks blood and in DMEM to ensure they are stable in the medium to treat the cells with them. The stability in the medium was checked for 3 days. They were stable in both PBS and DMEM as seen by the size distribution and by.PDI over the period of 3 days. The size distribution in PBS and DMEM is shown in figure (5c-5f). It's size was less than 200 nm in water at 4 ^{o}C at the end of one month suggesting that it has good shelf life (figure 5b).

3.1.2 Zeta Potential of NP3 in pH 5.5

NPs typically internalize into the cell via endosome pathway. The pH in lysosome is ~ 5.5. The NPs disassemble in the lysosome and the contents disseminate into the cytoplasm. The ZP of NP3 was measured in pH 5.5 solution. The ZP was 40.8 ± 0.5 mV. It was higher as compared to that in neutral conditions (35.1 ± 2.1 mV). However, it

remained similar over the period of 24 h. The increased value of ZP in pH 5.5 suggests that it may escape from lysosomes and home into mitochondria because of its high negative membrane potential which is ~ 150 mV.[31] This would minimize the unspecific distribution of drugs and concentrate the drugs in mitochondria which would increase the efficacy of drugs.

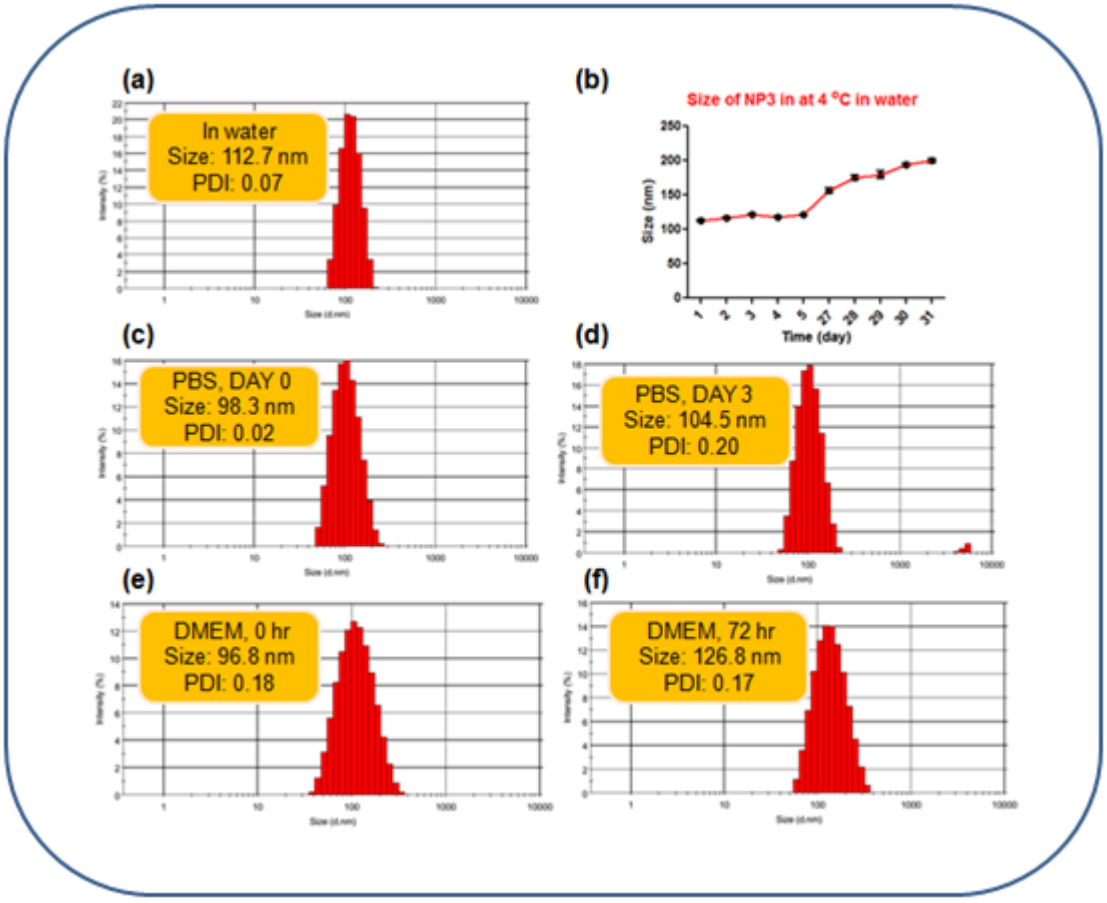

Figure 5: Size and stability of NP3 in water, PBS and DMEM. The average size and PDI are shown in the box

3.1.3 Quantification of drugs in NPs

Drug content in NP3 was determined by using UV-Vis spectroscopy. For camptothecin, the absorbance was measured at 367 nm in DMSO, for α-tocopheryl succinate at 288 nm in DMSO and for cisplatin at 706 nm in DMF solution of o-phenylenediamine. The data is shown in table 4 and represented in the bar diagram in figure 7.

The concentration of α-tocopheryl succinate was 3119.8 ± 780.9 μM, camptothecin was 232.4 ± 42.3 μM and of cisplatin was 439.5 ± 37.3 μM. .

Dilution	α-Tocopherol Succinate (μM)	Camptothecin (μM)	Dilution	Cisplatin (μM)
10	3400	238.2	20	441.6
15	3721.9	272.1	30	475.7
20	2237.5	186.9	40	401.1
Average	3119.8	232.4	Average	439.5
Std. Dev.	780.9	42.3	Std. Dev.	37.3

Table 4: Drug loading in NP3

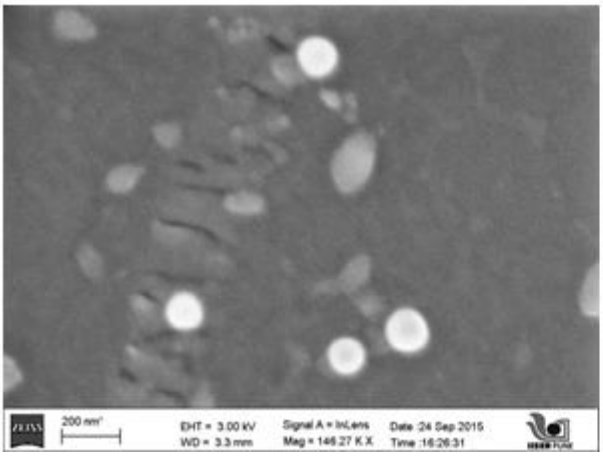

Figure 6: FESEM image of NP3

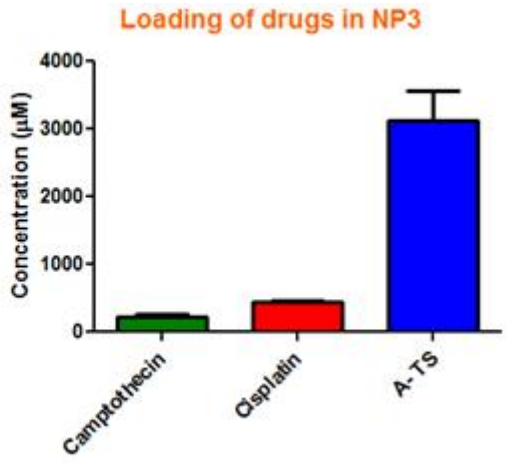

Figure 7: Drug loading in NP3

3.2 Studies on the tertiary amine-functionalized nanoparticles

As mentioned in the introduction that delocalized lipophilic cations and MPPs are used to deliver the drugs to mitochondria. But their homing into mitochondria is not well understood. To determine the factors that home a molecule into mitochondria, we synthesized tertiary amine molecules based positively charged compounds with α-tocopheryl succinate (**8**), (**9**), (**10**) and (**11**). The library of compounds is very small and will be expanded to generalize any factor that effects the homing into mitochondria. We synthesized the nanoparticles with (**8**), (**9**) and (**11**).

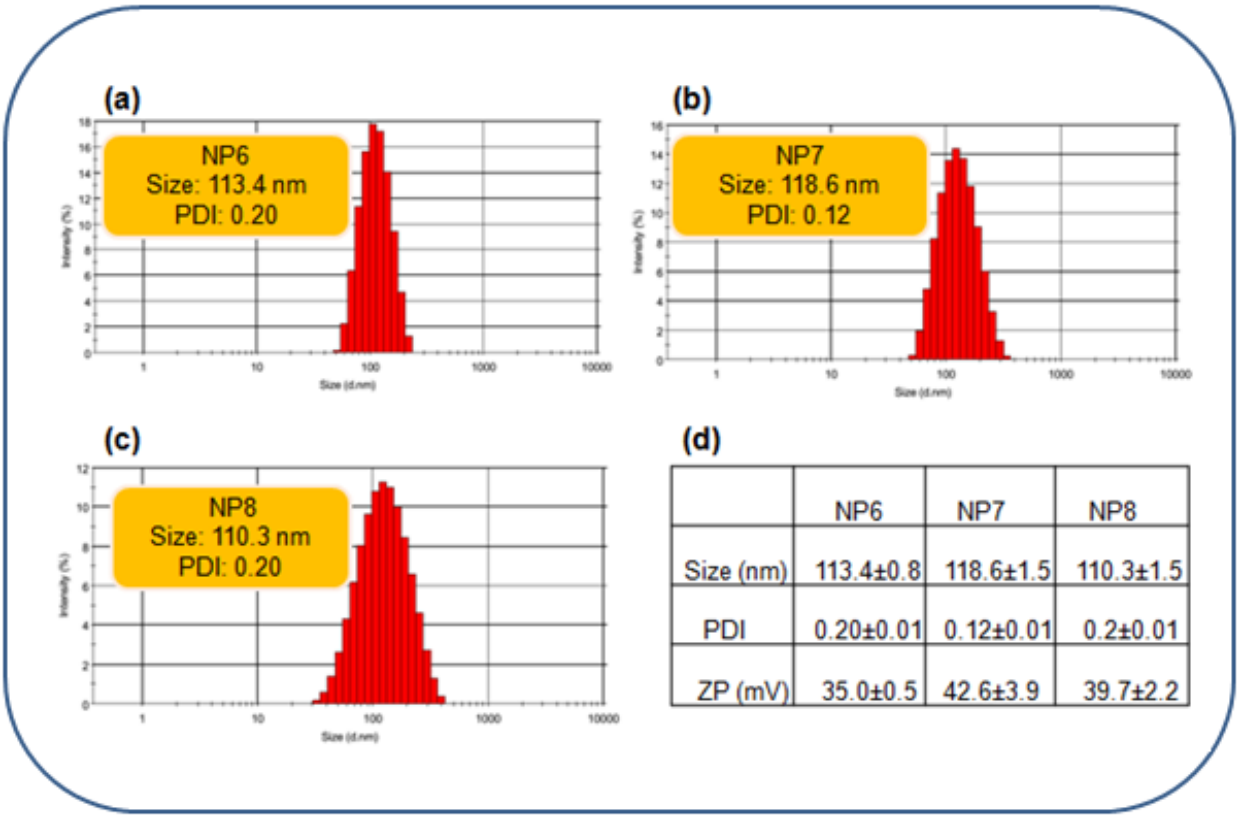

Figure 8: Size distribution, PDI and ZP of tertiary amine-functionalized nanoparticles.

It is encouraging that they could be engineered into a nanoparticle with the size that is desirable for biological applications.[7] The nanoparticles are monodisperse as suggested by their size distribution and PDI values. The ZP values indicate that the nanoparticles are positively charged. Their average ZP values are > 35 mV. It is reported that the nanoparticles with ZP values > 30 mV home into mitochondria.[19,20] Taking only ZP values into consideration, these nanoparticles would home into mitochondria. However, the homing would depend on the delocalization of charge as the delocalized charge would require little desolvation energy when the nanoparticles would desolvate to permeate the highly hydrophobic mitochondrial membrane. Homing into mitochondria also depends on the hydrophobicity of the molecule as it would have to permeate highly hydrophobic mitochondrial membrane.[45] To conclude anything about the homing of nanoparticles into mitochondria, the library of nanoparticles needs to be expanded taking into account the charge delocalization and hydrophobicity. The size distribution, size, PDI and ZP are shown in the figure (8).

3.3 Effect of sonication on the size and PDI of NPs

We wanted to see how sonication would effect the size and polydispersity of nanoparticles and if we can tune the size of nanoparticles by sonication. For this experiment, a previously synthesized nanoparticle NP3 was used. It was stored for over 2 months at 4 ^{o}C. Its size was ~ 400 nm and PDI 0.63 as determined by DLS. It was sonicated for varying amount of time and the effect on size and PDI was observed.

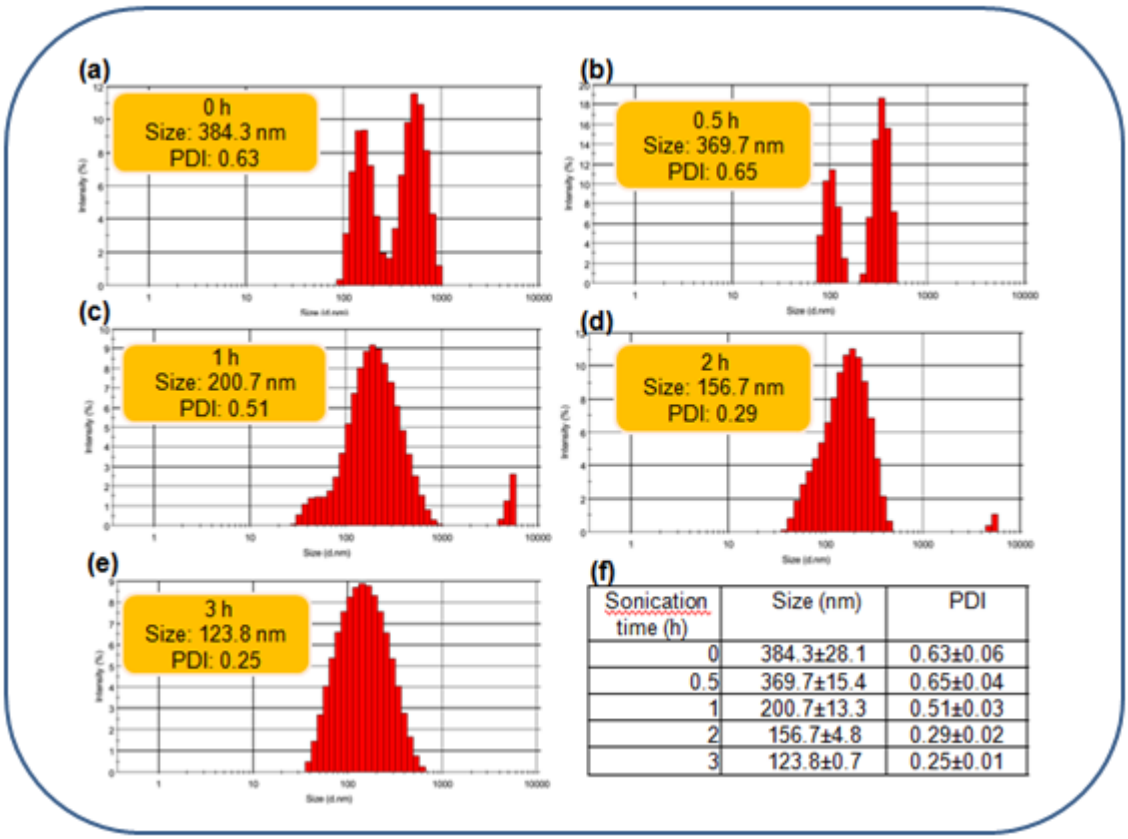

Sonication time (h)	Size (nm)	PDI
0	384.3±28.1	0.63±0.06
0.5	369.7±15.4	0.65±0.04
1	200.7±13.3	0.51±0.03
2	156.7±4.8	0.29±0.02
3	123.8±0.7	0.25±0.01

.

Figure 9: Effect of sonication time on nanoparticle size and polydispersity. Size distribution, size and PDI values are shown.

It was observed that with increase in sonication time, size and PDI of the nanoparticle both decreased (figure 9, 10). The size was ~ 125 nm and PDI was 0.25 after 3 hr sonication. Thus they decreased in size and became more monodisperse. The drug loading was not checked after sonication. However, it is expected to be same as earlier as the components of the nanoparticle were all hydrophobic. They would reorganize into a nanoparticle. The results are very encouraging as the bigger size nanoparticles can

be decreased to smaller nanoparticles with increased monodispersity. We can now decrease the size of NP1 (432.4 nm) and NP2 (283.5 nm) by sonication and study them further. If we could obtain smaller nanoparticles of NP1 and NP2, we would be able to explore the anti-cancer efficacy of nanoparticles (NP1, NP2 and NP3) with varying amounts of three drugs encapsulated. We will check the effect of sonication on drug loading and see if it remains the same. In case it does not, it can be used to engineer nanoparticles with varying drug content of the same nanoparticles.

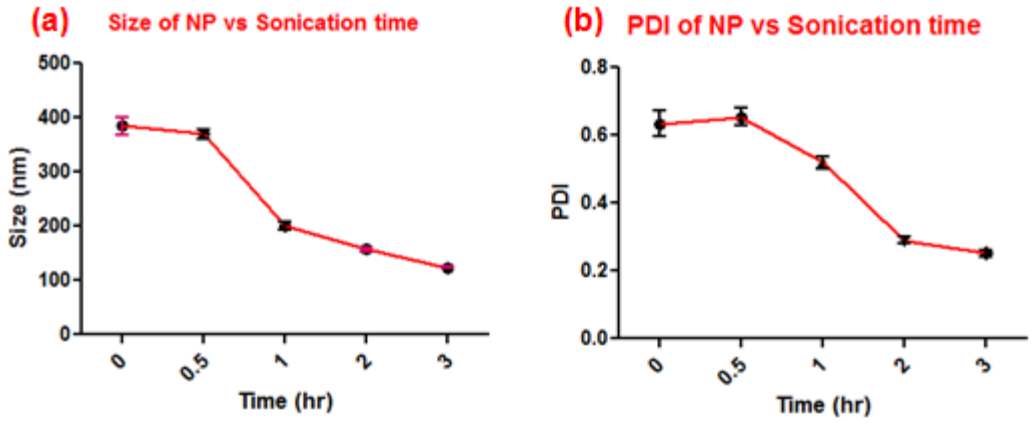

Figure 10: Variation of size (a) and PDI (b) of nanoparticles with sonication time.

Conclusion

To deliver the mitochondria damaging drugs to mitochondria and to increase the efficacy of drugs, positively charged nanoparticles containing three drugs were engineered. The nanoparticles were spherical in shape, about 115 nm in size and monodisperse with the zeta potential value of 35 mV. NPs were stable in PBS at 37 ^{o}C and DMEM for 3 days and were < 200 nm in water at 4 ^{o}C after 30 days. Its zeta potential value increased to 40 mV in pH 5.5 but remained similar over 24 h. The nanoparticles are being evaluated for their efficacy in various cancer cell lines. Further, its mechanism of action will be studied. Tertiary amine-functionalized nanoparticles were engineered to understand the factors affecting mitochondrial localization. The nanoparticles were all < 120 nm in size and monodisperse. Their zeta potential values were > 35 mV. The set of these nanoparticles will be expanded and their mitochondrial localization will be studied.

References

(1) Holohan, C.; Schaeybroeck, S. V.; Longley, D. B.; Johnston, P. G. *Nat. Rev. Cancer* **2013**, *13*, 714-726.

(2) Coburn, J. M.; Kaplan, D. L. *Bioconjugate Chem.* **2015**, *26 (7)*, 1212-1223.

(3) Hanahan, D.; Weinberg, R. A. *Cell* **2000**, *100,* 57-70.

(4) Hanahan, D.; Weinberg, R. A. *Cell* **2011**, *144,* 646-674.

(5) Siddik, Z. H. *Oncogene* **2003**, *22*, 7265-7267.

(6) Tacar, O.; Sriamornsak, P.; Dass, C. R. *J. Pharm. Pharmacol.* **2013**, *65*, 157-170.

(7) Peer, D.; Karp, J. M.; Hong, S.; Farokhzad, O. C.; Margalit, R.; Langer, R. *Nat. Nanotechnol* **2007**, *2*, 751-760.

(8) Biswas, S.; Torchilin, V. P. *Adv. Drug Deliv. Rev* **2014**, *66*, 26-41.

(9) Mura, S.; Nicolas, J.; Couvreur, P. *Nat. Mater* **2013**, *12*, 91-1003.

(10) Sengupta, P.; Basu, S.; Soni, S.; Pandey, A.; Roy, B.; Oh, M. S.; Chin, K. T.; Paraskar, A. S.; Sarangi, S.; Connor, Y.; Sabbisth, V. S.; Koapparam, J.; Kulkarni, A.; Muto, K.; Amarasiriwardena, C.; Jayawardene, I.; Lupoli, N.; Dinulescu, D. M.; Bonventre, J. V.; Mashelkar R. A.; Sengupta, S. *Proc. Natl. Acad. Sci. U.S. A.* **2012**, *109 (28)*, 11294-11299.

(11) Patil, S.; Patil, S.; Gawali, S.; Shende, S.; Jadhav, S.; Basu, S. *RSC Adv.* **2013**, *3*, 19760-19764.

(12) Patil, S.; Gawali, S. Patil, S.; Basu, S. *J. Mater. Chem. B* **2013**, *1*, 5742-5750.

(13) Correia, A.; Shahbazi, M. A.; Makila, E.; Almeida, S.; Salonen, J.; Hirvonen, J.; Santos, H. A. *ACS Appl. Mater. Interfaces* **2015**, *7 (41)*, 23197-23204.

(14) Lobovkina, T.; Jacobsen, G. B.; Gonzalez, E. Z.; Hickerson, R. P.; Leake, D.; Kaspar, R. L.; Contag, C. H.; Zare, R. N. *ACS Nano* **2011**, *5 (12)*, 9977-9983.

(15) Paraskar, A.; Soni, S.; Basu, S.; Amarasiriwardena, C. J.; Srivats, S.; Roy, R. S.; Sengupta, S. *Nanotechnology* **2011**, *22*, 265101.

(16) Wang, J.; Liu, W.; Tu, Q.; Wang, J.; Song, N.; Zhang, Y.; Nie, N.; Wang, J. *Biomacromolecules* **2011**, *12 (1)*, 228-234.

(17) Mauro, N.; Scialabba, C.; Cavallaro, G. Licciardi, M.; Giammona, G. *Biomacromolecules* **2015**, *16 (9)*, 2766-2775.

(18) Qiu, L.; Chen, T.; Ocsoy, I.; Yasun, E.; Wu, C.; Zhu, G.; You, M.; Han, D.; Jiang, J.; Yu, R.; Tan, W. *Nano Lett.* **2015**, *15*, 457-463.

(19) Marrache, S.; Dhar, S. *Proc. Natl. Acad. Sci. U.S.A.* **2012**, *109 (40)*, 16288-17293.

(20) Mallick, A.; More, P.; Syed, M. M. K.; Basu, S. *(Under Review)*

(21) Dhar, S.; Kolishetti, N.; Lippard, S. J.; Farokhzad, O. C. *Proc. Natl. Acad. Sci. U.S.A.* **2011**, *108 (5)*, 1850-1855.

(22) Poon, Z.; Lee, J. B.; Morton, S. W.; Hammond, P. T. *Nano Lett.* **2011**, *11 (5)*, 2096-2103.

(23) Liao, L.; Liu, J.; Dreaden, E. C.; Morton, S. W.; Shopsowitz, K. E.; Hammond, P. T.; Johnson, J. A. *J. Am. Chem. Soc.* **2014**, *136*, 5896-5899.

(24) Mallick, A.; More, P.; Ghosh, S.; Chippalkatti, R.; Chopade, B. A.; Lahiri, M.; Basu, S. *ACS Appl Mater Interfaces* **2015**, *7 (14)*, 7584-7598.

(25) Palvai, S.; More, P.; Mapara, N.; Basu, S. *ACS Appl. Mater. Interfaces* **2015**, *7 (33)*, 18327-18335.

(26) Palvai, S.; More, P.; Mapara, N.; Nagraj, J.; Chowdhury, R.; Basu, S. *ChemNanoMat* **2016**, *2*, 201-211.

(27) Wisnovsky, S. P.; Wilson, J. J.; Radford, R. J.; Pereira, M. P.; Chan, M. R.; Laposa, R. R.; Lippards, S. J.; Kelley, S. O. *Chem. Biol.* **2013**, *20*, 1323-1328.

(28) Chamberlain, G. R.; Tulumello, D. V.; Kelley, S. O. *ACS Chem. Biol.* **2013**, *8*, 1389-1395.

(29) Fonseca, S. B.; Pereira, M. P.; Mourtada, R.; Gronda, M.; Horton, K. L.; Hurren, R.; Minden, M. D.; Schimmer, A. D.; Kelley, S. O. *Chem. Biol.* **2011**, *18*, 445-453.

(30) Marrache, S.; Pathank, R. K.; Dhar, S. *Proc. Natl. Acad. Sci. U.S.A.* **2014**, *111 (29)*, 10444-10449.

(31) Fulda, S.; Galluzzi, L.; Kroemer, G. *Nat. Rev. Drug Discovery* **2010**, *9*, 447-464.

(32) Weinberg, S. E.; Chandel, N. S. *Nat. Chem. Biol.* **2014**, *11*, 9-15.

(33) Qu, Q.; Ma, X.; Zhao, Y. *Nanoscale* **2015**, *7*, 16677-16686.

(34) Wang, L.; Liu, Y.; Li, W.; Jiang, X.; Ji, Y.; Wu, X.; Xu, L.; Qiu, Y.; Zhao, K.;

Wei, T.; Li, Y.; Zhao, Y.; Chen C. *Nano Lett.* **2011**, *11*, 772-780.

(35) Chan, M. S.; Tam, D. Y.; Dai, Z.; Liu, L. S.; Ho, J. W-T.; Chan, M. L.; Xu, D.; Wong, M. S.; Tin, C.; Lo, P. K. *Small* **2016**, *12 (6)*, 770-781.

(36) Attardi, G.; Schatz, G. *Annu. Rev. Cell Dev. Biol.* **1988**, *4*, 289-331.

(37) Johnstone, J.C.; Suntharalingam, K.; Lippard, S. J. *Chem. Rev.* **2016**, *116 (5)*, 3436-3486.

(38) Paraskar, A. S.; Soni, S.; Chin, K. T.; Chaudhuri, P.; Muto, K. W.; Berkowitz, J,; Handlogten, M. W.; Alves, N. J.; Bilgicer, B.; Dinulescu, D. M.; Mashelkar, R. A.; Sengupta, S. *Proc. Natl. Acad. Sci. U.S.A.* **2010**, *107 (28)*, 12435-12440.

(39) Ling, X.; Shen, Y.; Sun, R.; Zhang, M.; Li, C.; Mao, J.; Xing, J.; Sun, C.; Tu, J. *Polym. Chem.* **2015**, *6*, 1541-1552.

(40) Verma, R. P.; Hansch, C. *Chem. Rev.* **2009**, *109*, 213-235.

(41) Cheng, J.; Khin, K. T.; Davis, M. E. *Mol. Pharm.* **2004**, *1*, 183-193.

(42) Xiao, B.; Si, X.; Han, M. W.; Viennois, E.; Zhang, M.; Merlin, D. *J. Mater. Chem. B* **2015**, *3*, 7724-7733.

(43) Pramod, P. S.; Shah, R.; Sonali, C.; Balasubramanian, N.; Jayakannan, M. *Nanoscale* **2014**, *6*, 11841-11855.

(44) Dang, X. F.; Low, P.; Dyason, J. C.; Wang, X. F.; Prochazka, L.; Witting, P. K.; Freeman, R.; Swettenham, E.; Valis, K.; Liu, J.; Zobalova, R.; Turanek, J.; Spitz, D. R.; Domann, F. E.; Scheffler, I. E.; Ralph, S. J.; Neuzil, J. *Oncogene* **2008**, *27*, 4324-4335.

(45) Jean, S. R.; Tulumello, D. V.; Wisnovsky, S. P.; Lei, E. K.; Pereira, M. P.; Kelley, S. O. *ACS Chem. Biol.* **2014**, *9*, 323-333.

Appendix: Characterization Data

^{1}H NMR (400 MHz, $CDCl_3$) (3)

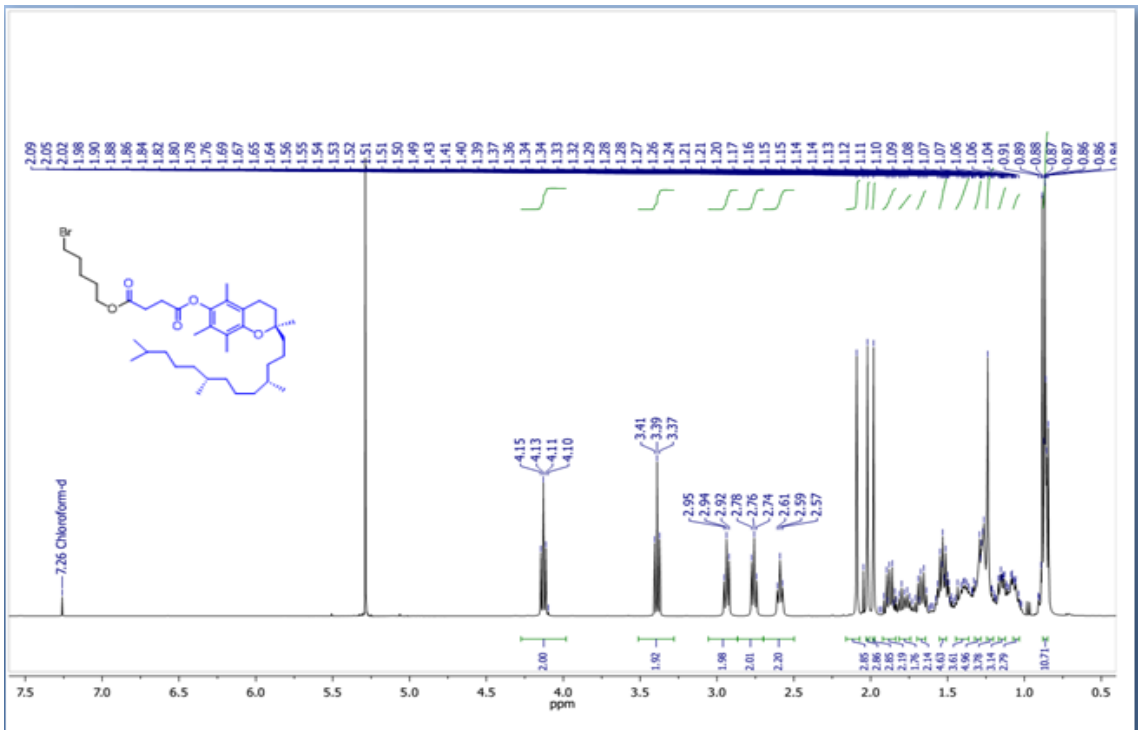

^{13}C NMR (100 MHz, $CDCl_3$) (3)

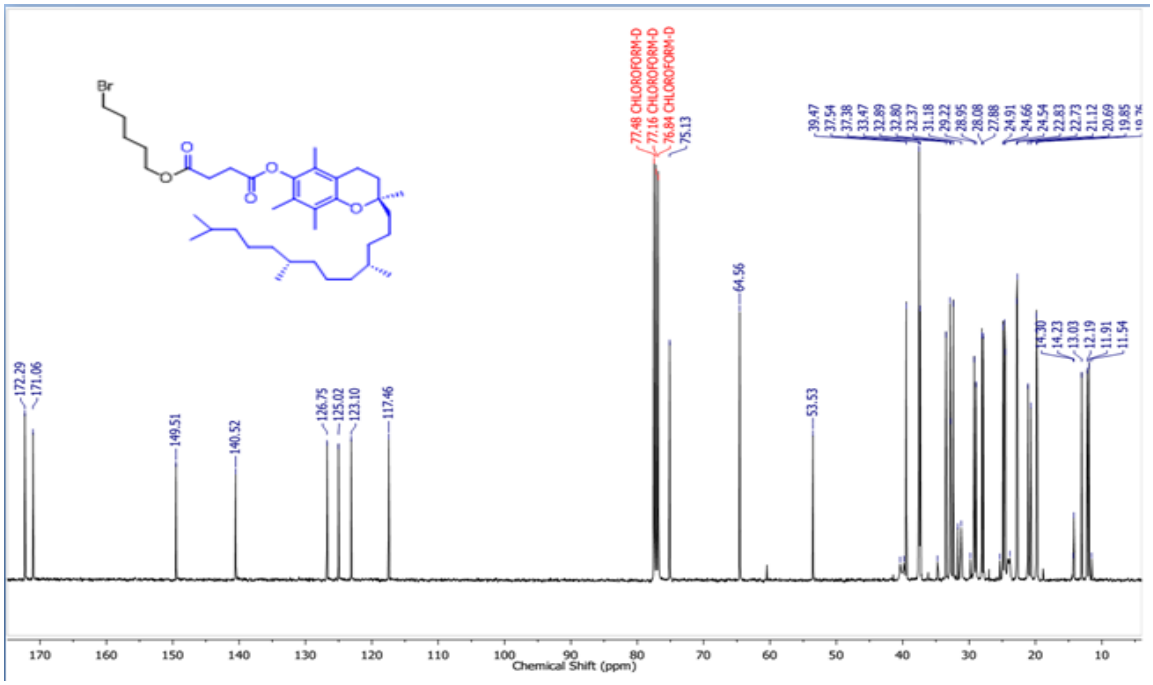

^{1}H NMR (400 MHz, $CDCl_3$) (4)

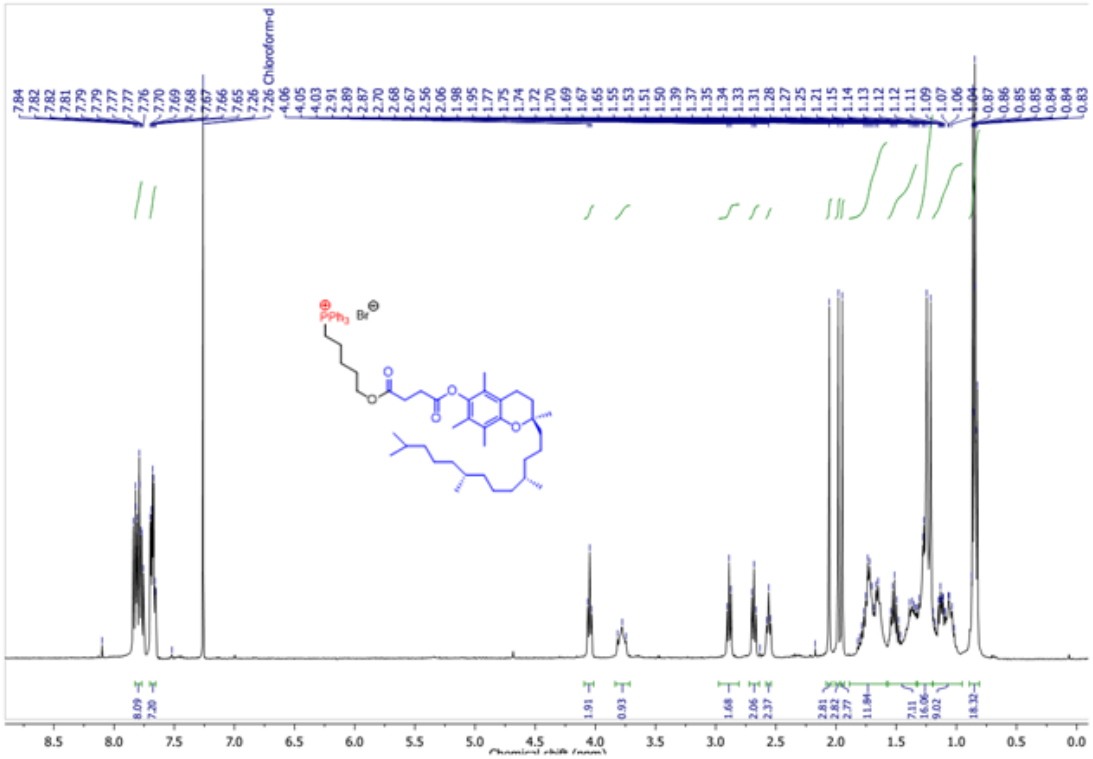

^{13}C NMR (100 MHz, $CDCl_3$) (4)

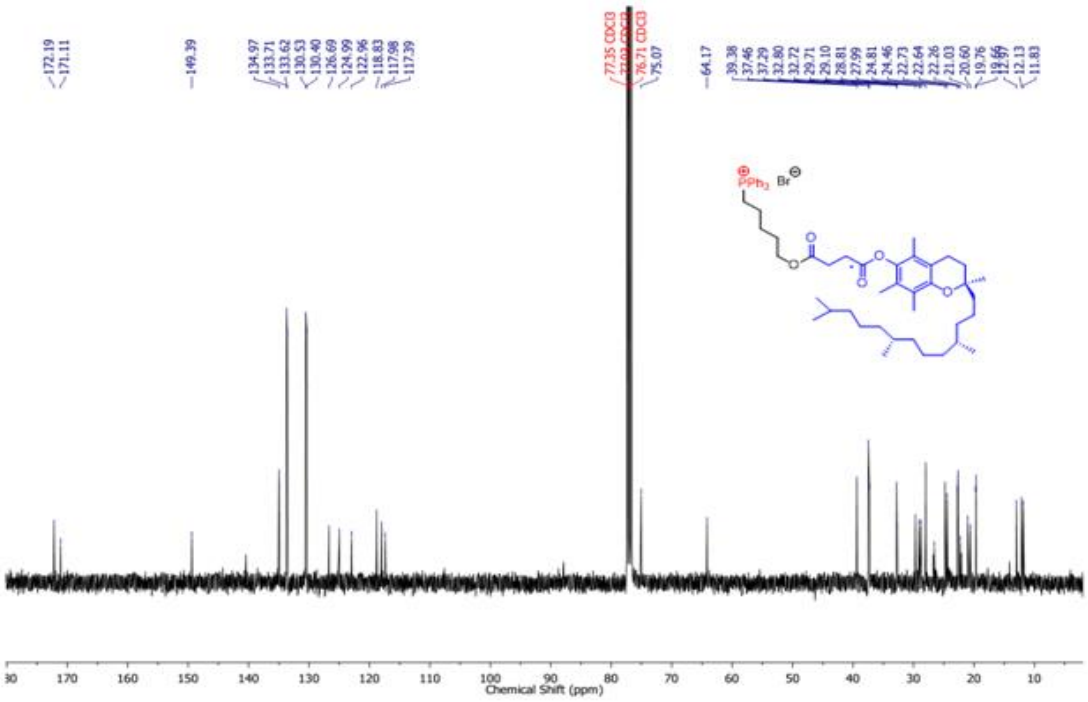

^{1}H NMR (400 MHz, $CDCl_3$) (7)

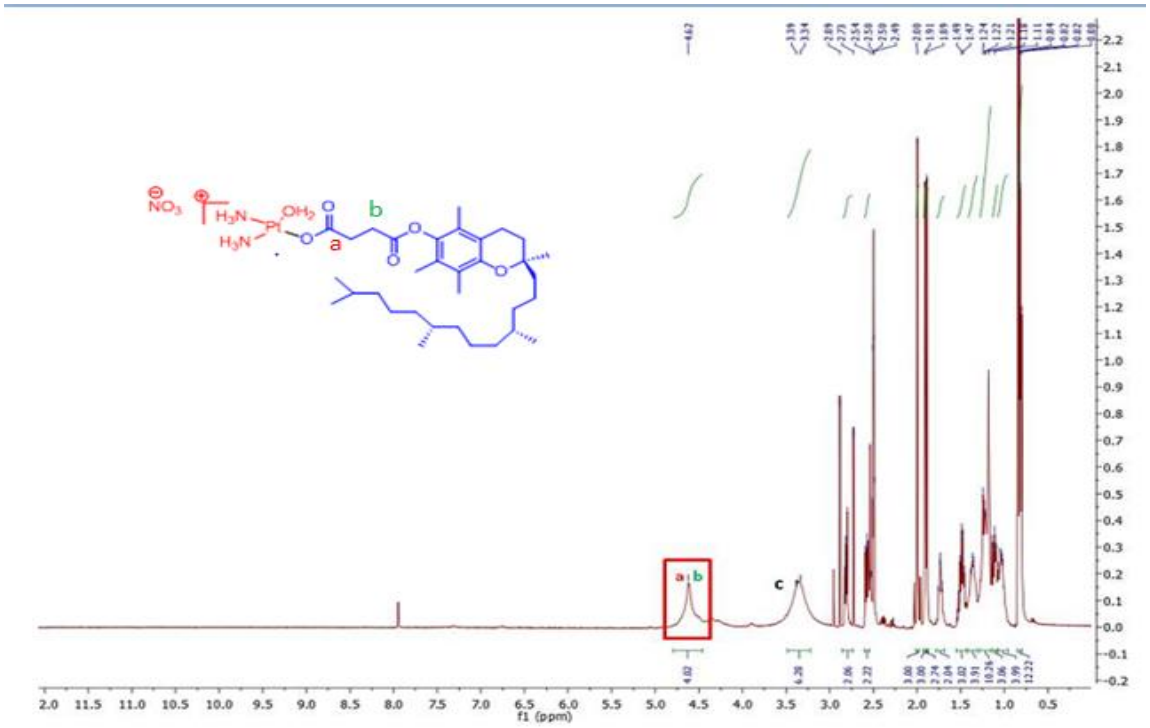

^{13}C NMR (100 MHz, $CDCl_3$) (7)

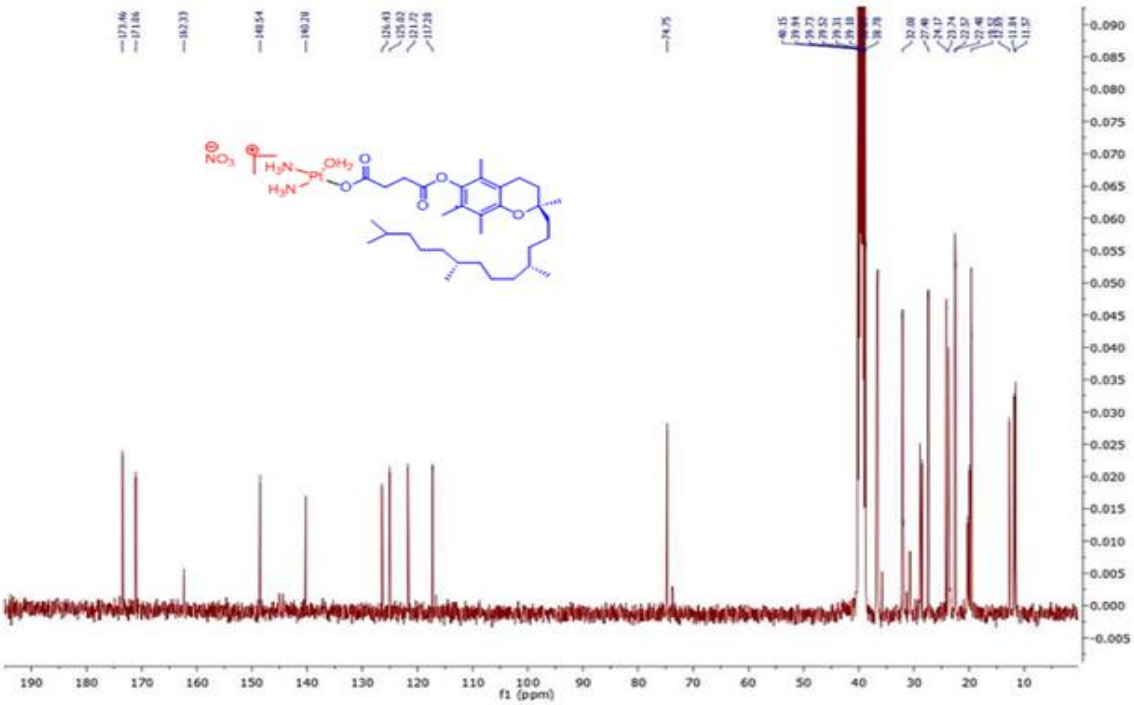

^{195} Pt NMR (7)

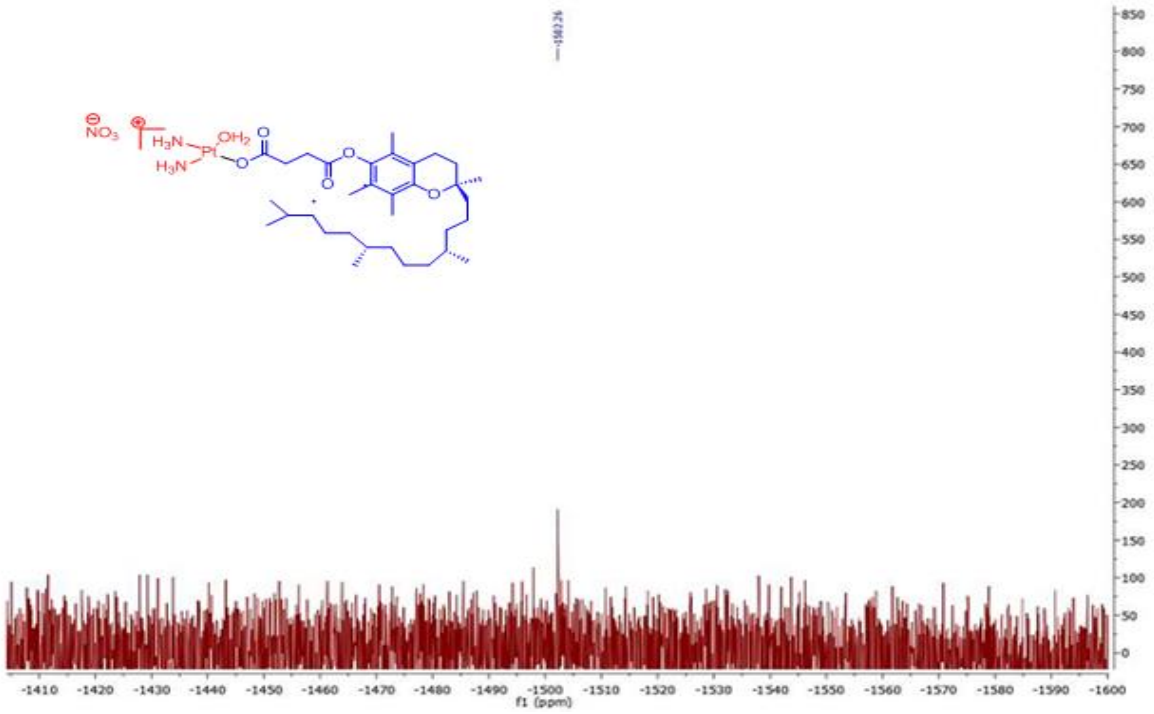

^{1}H NMR (400 MHz, $CDCl_3$) (8)

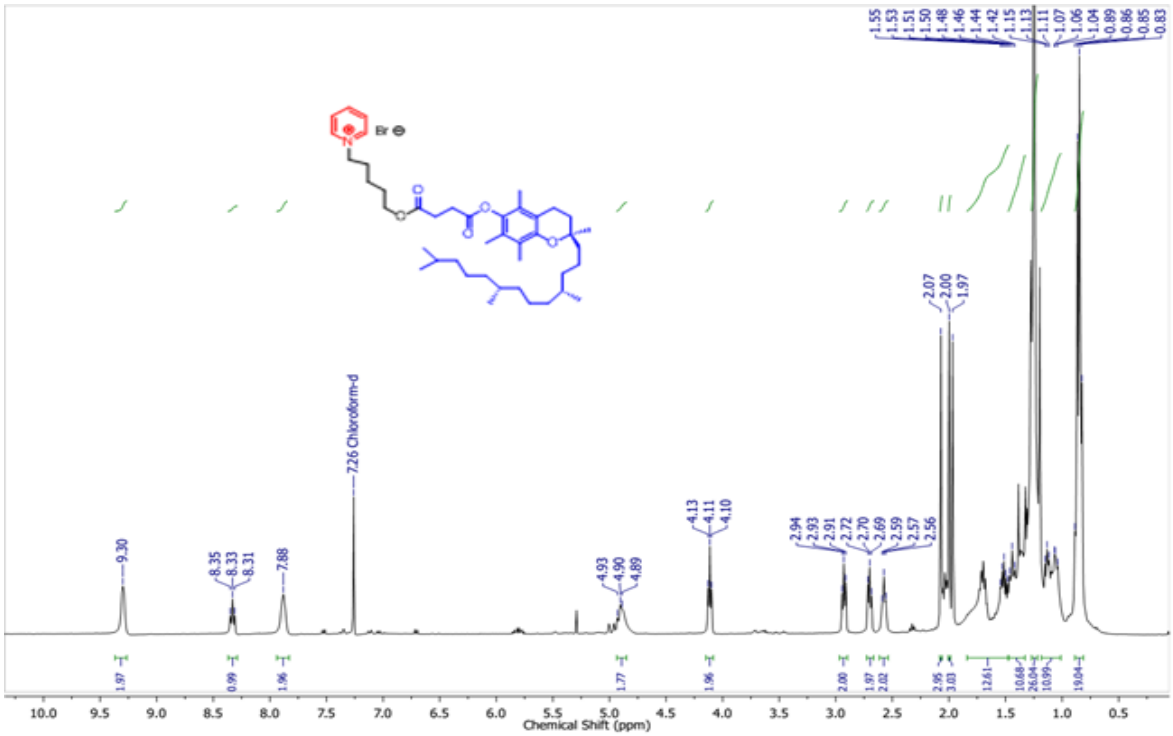

^{13}C NMR (100 MHz, $CDCl_3$) (8)

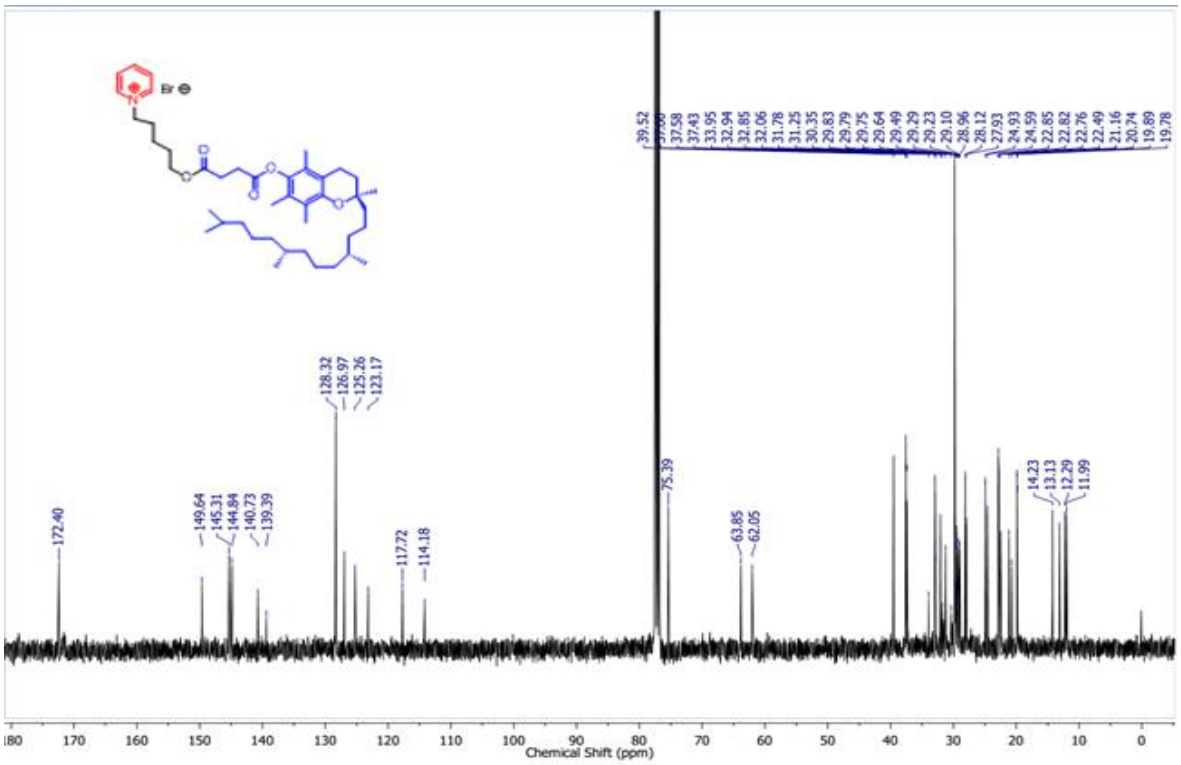

HRMS (ESI) (8)

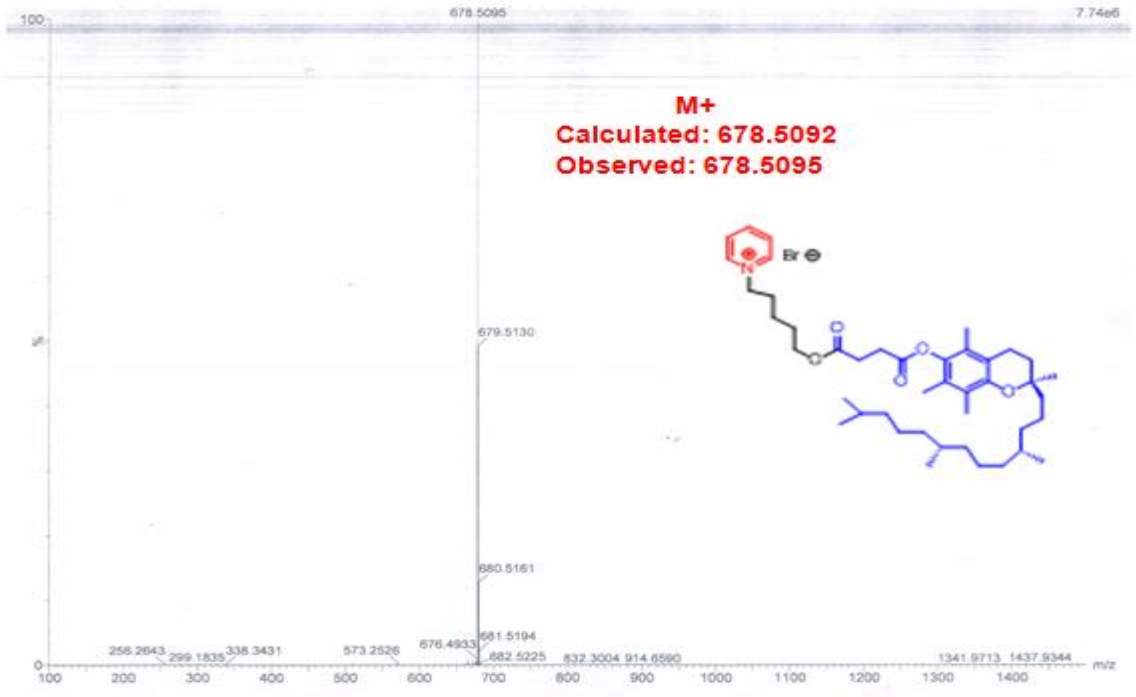

^{1}H NMR (400 MHz, $CDCl_3$) (9)

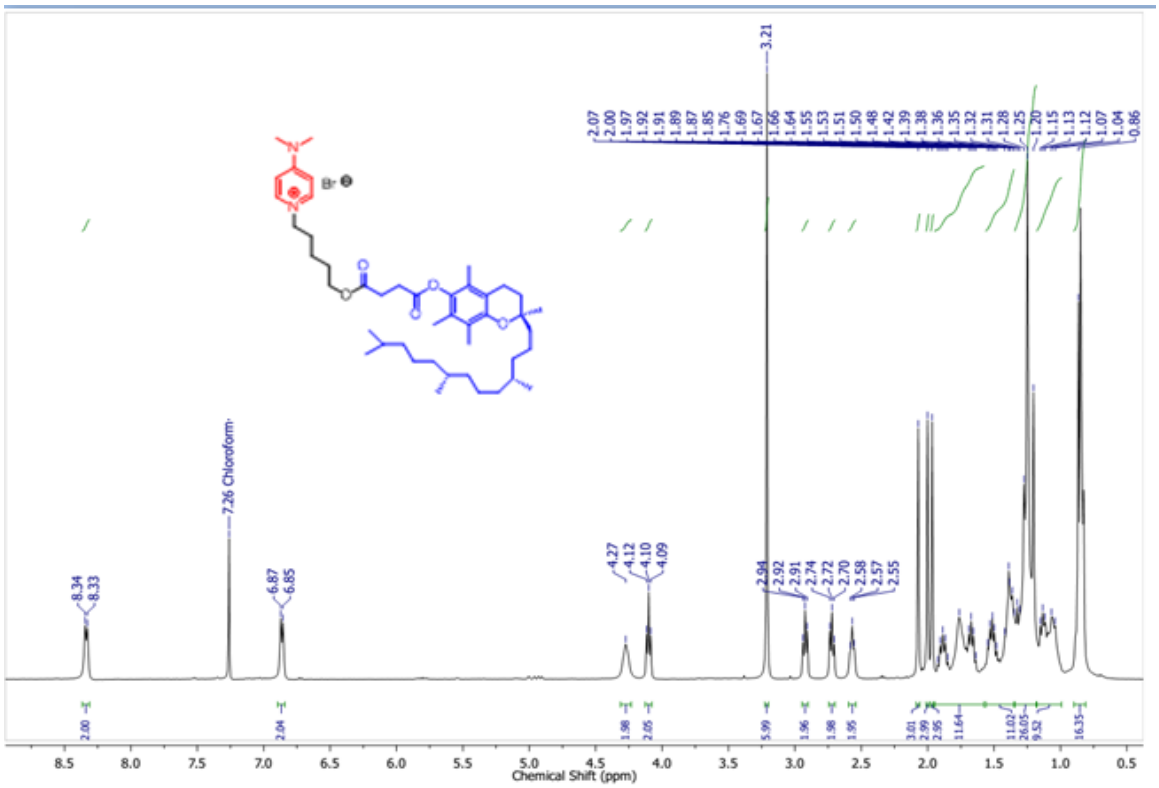

^{13}C NMR (100 MHz, $CDCl_3$) (9)

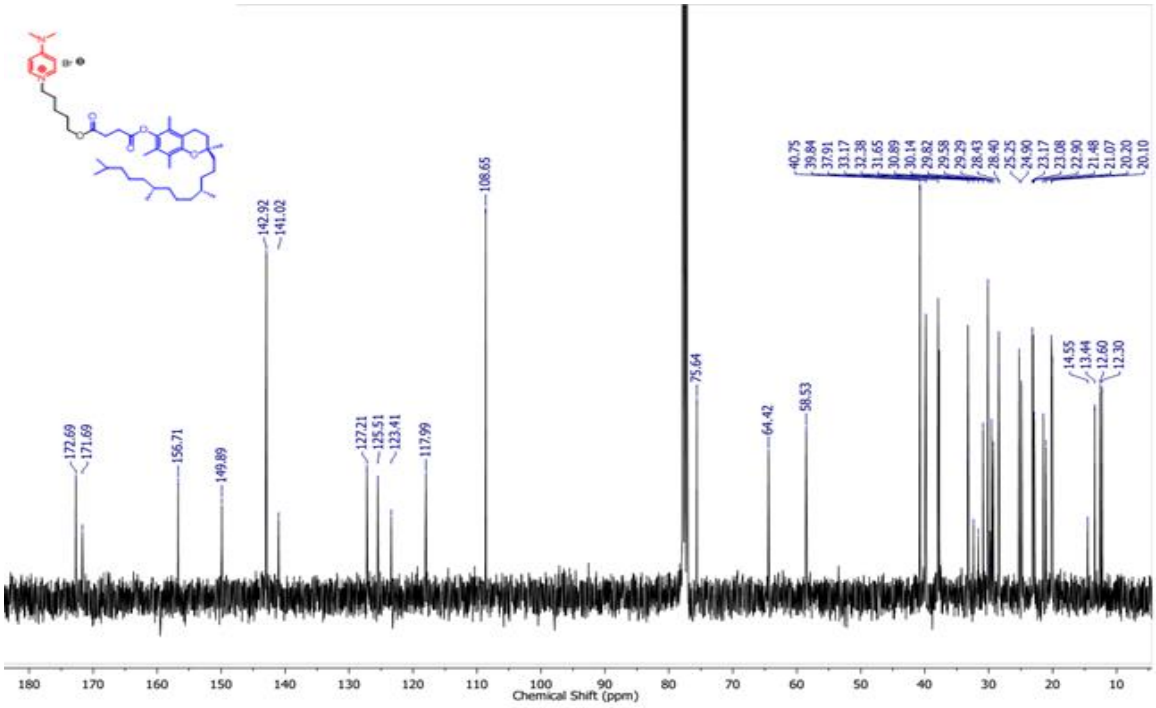

HRMS (ESI) (9)

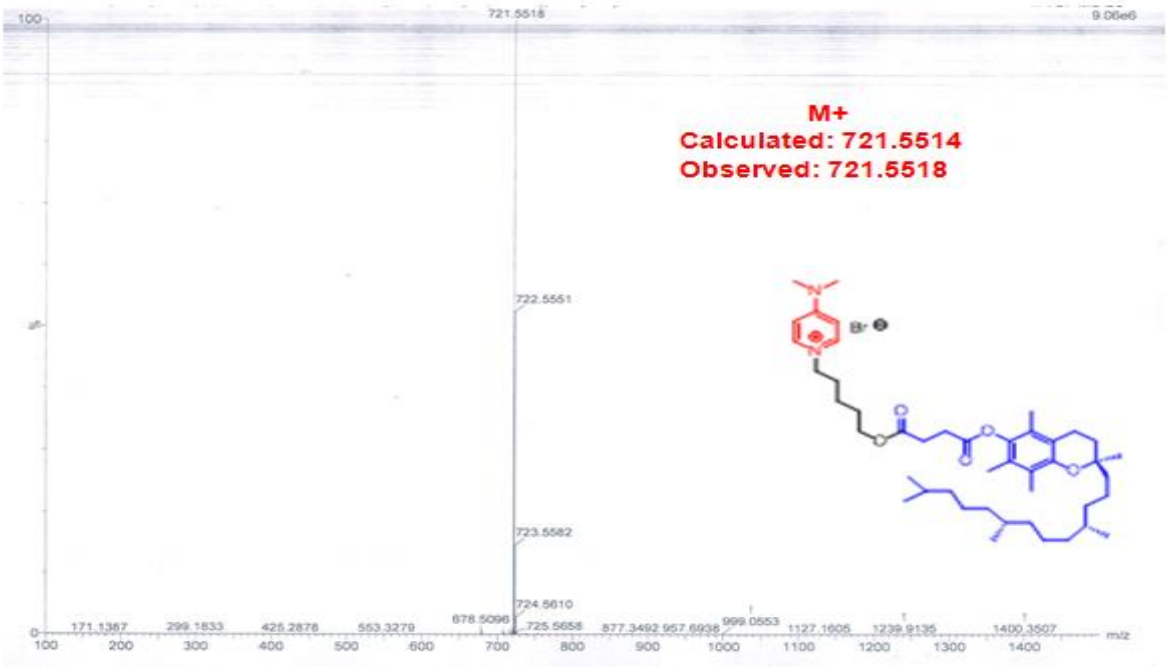

^{1}H NMR (400 MHz, $CDCl_3$) (10)

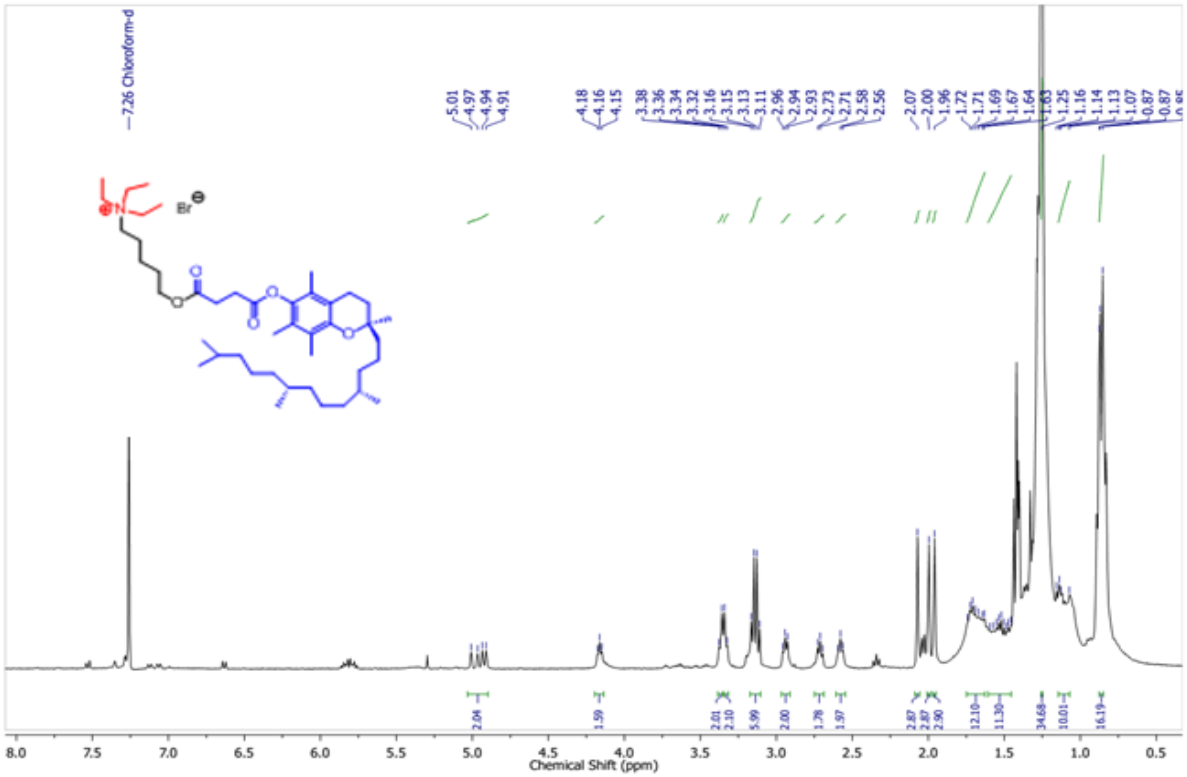

^{13}C NMR (100 MHz, $CDCl_3$) (10)

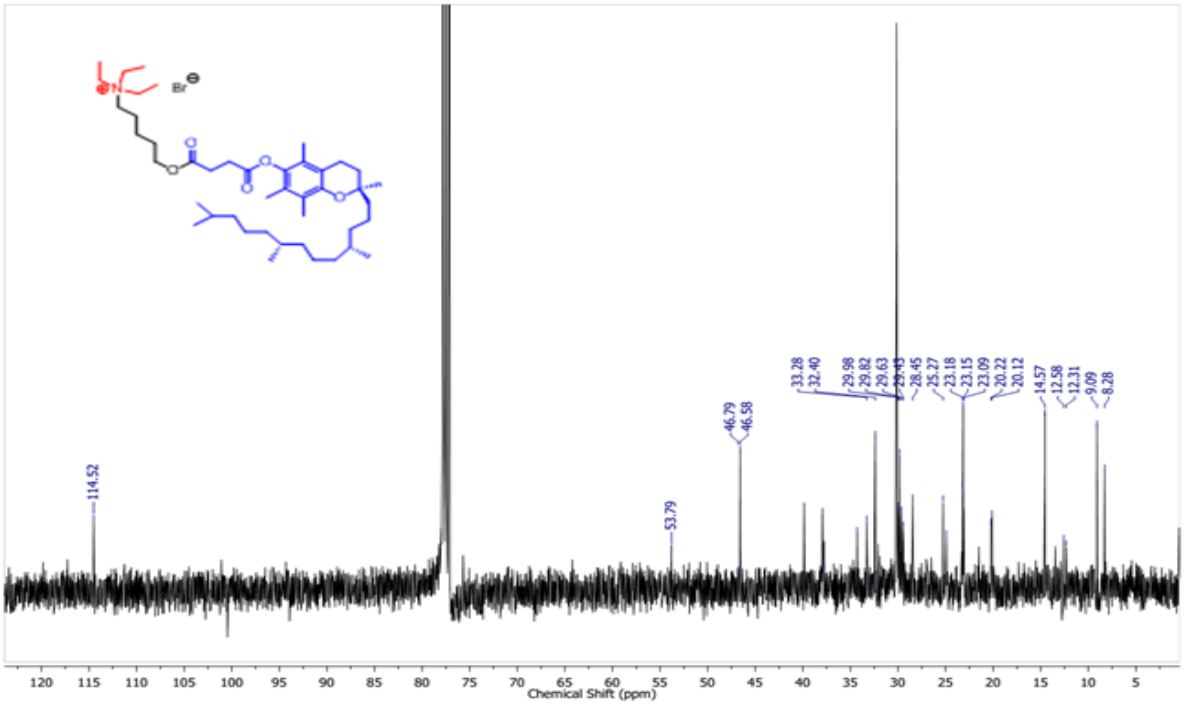

HRMS (ESI) (10)

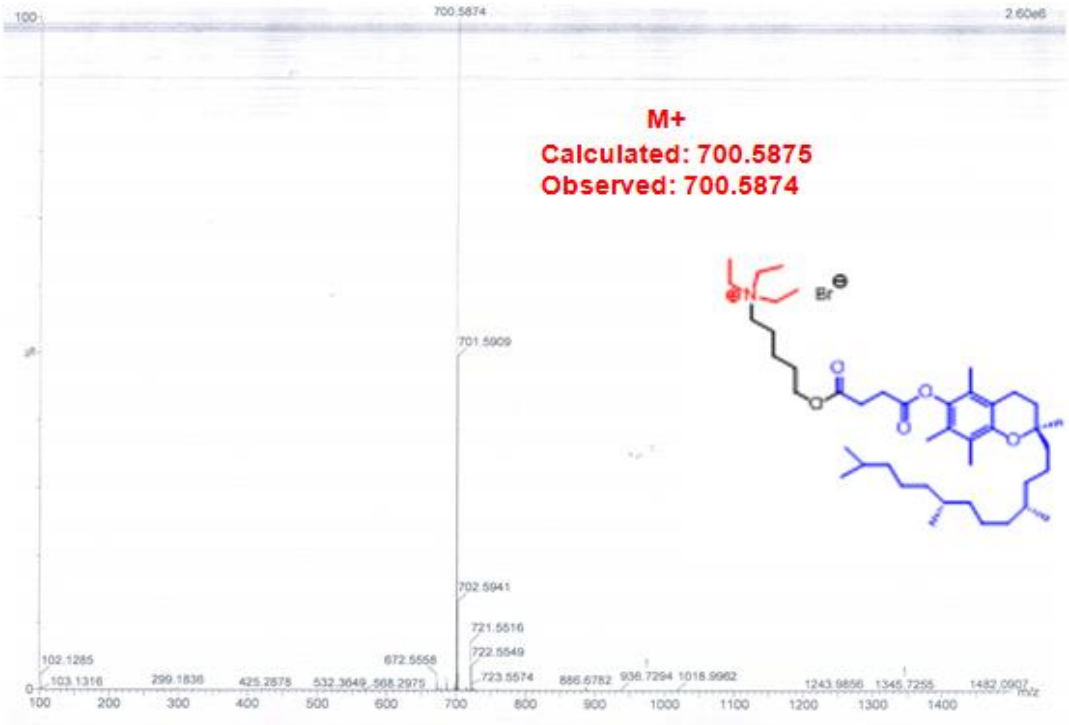

^{1}H NMR (400 MHz, $CDCl_3$) (11)

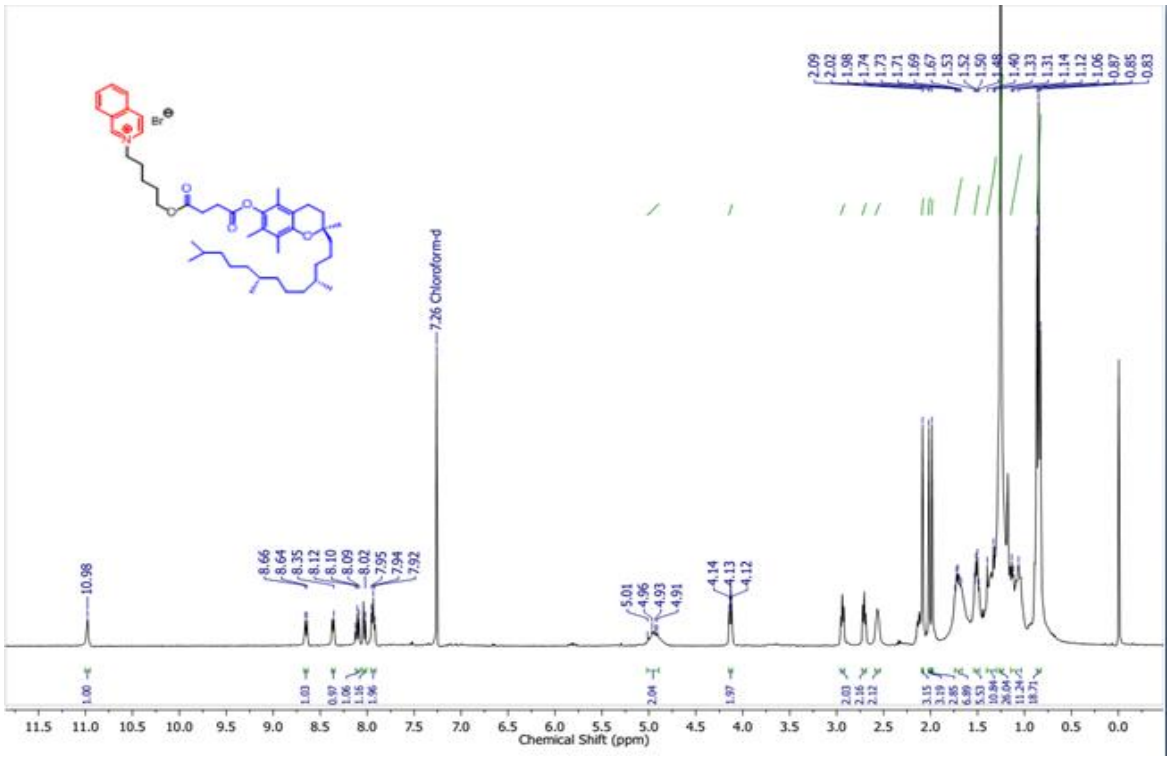

^{13}C NMR (100 MHz, $CDCl_3$) (11)

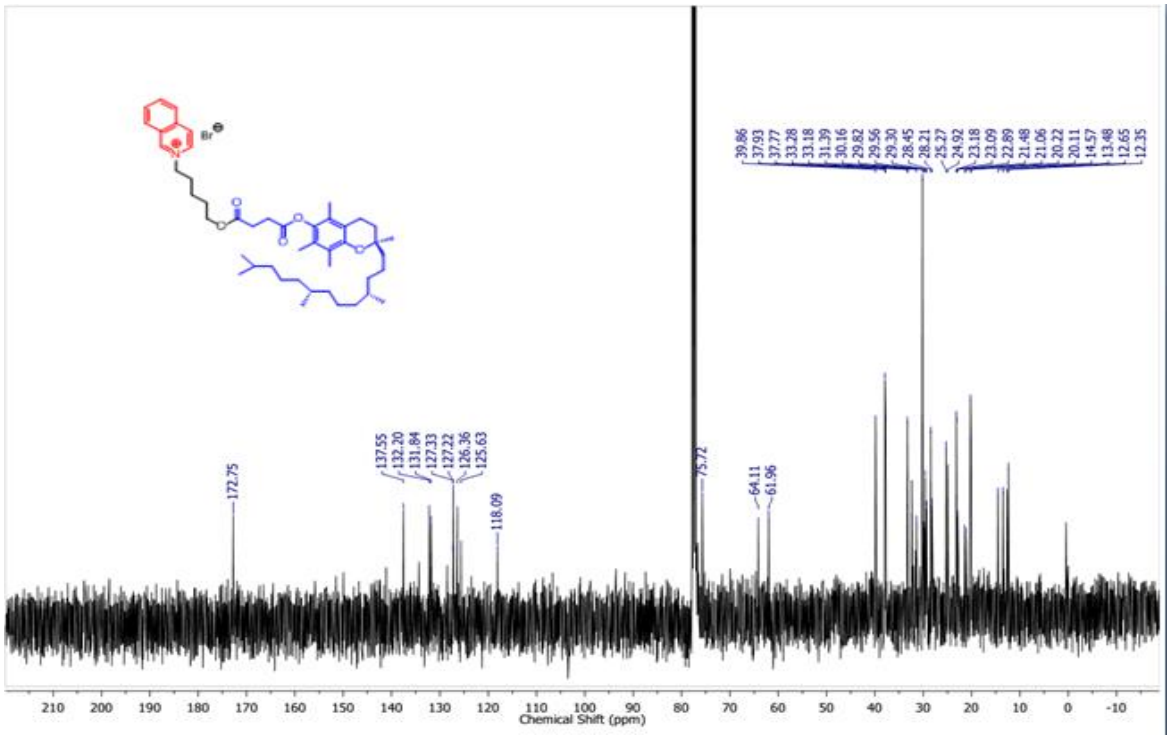

HRMS (ESI) (11)

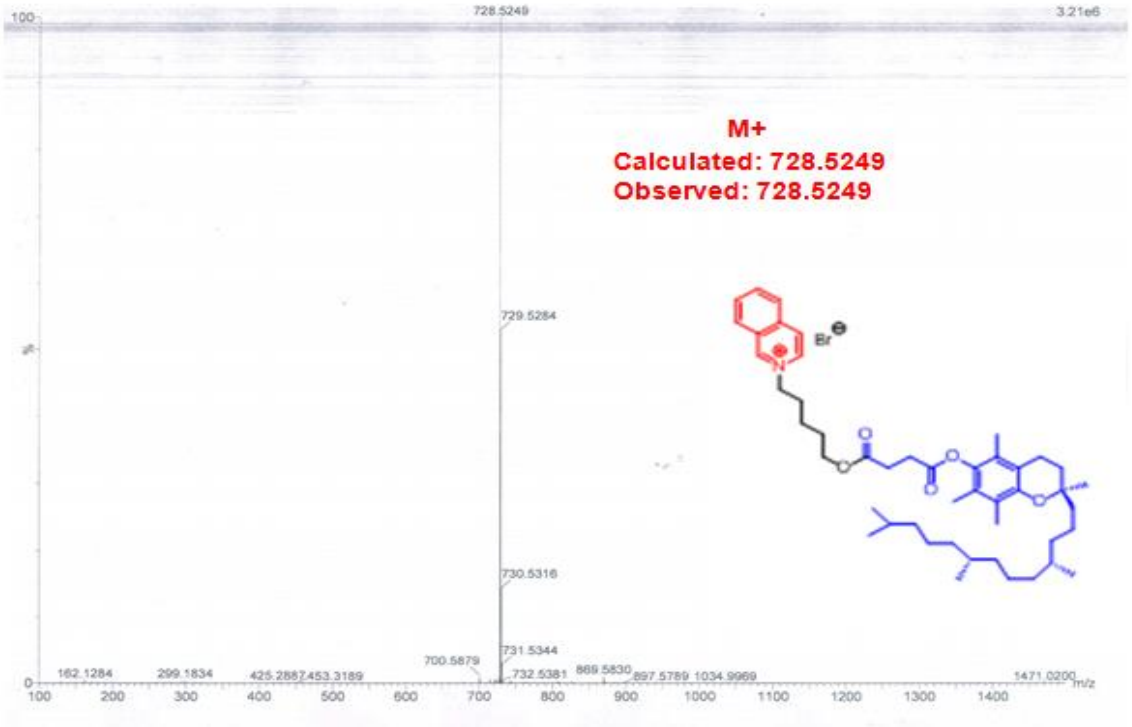

^{1}H NMR (400 MHz, DMSO-d6) (16)

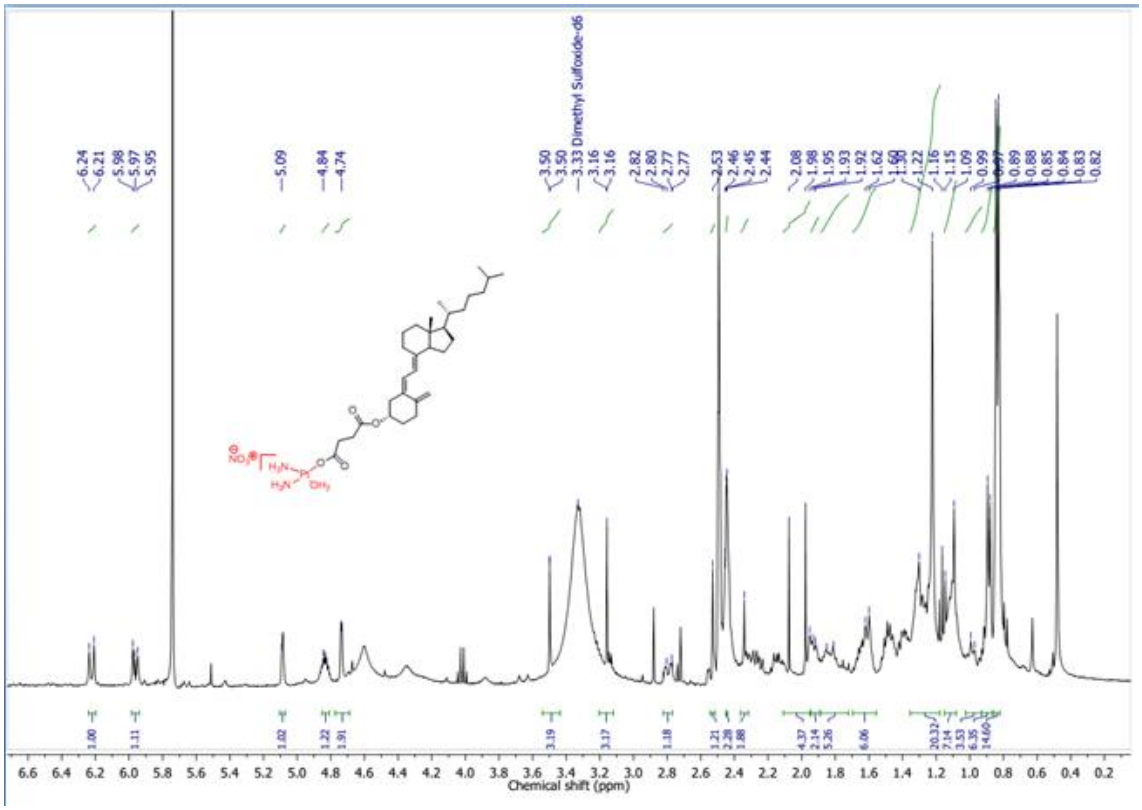

^{13}C NMR (100 MHz, DMSO-d6) (16)

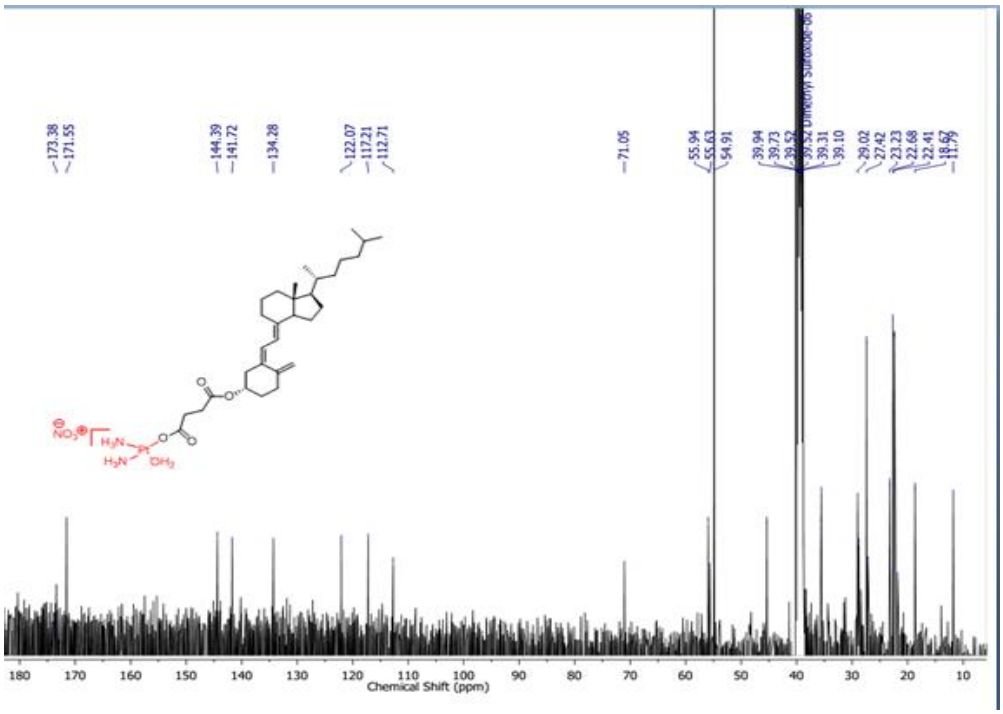

^{1}H NMR (400 MHz, $CDCl_3$) (18)

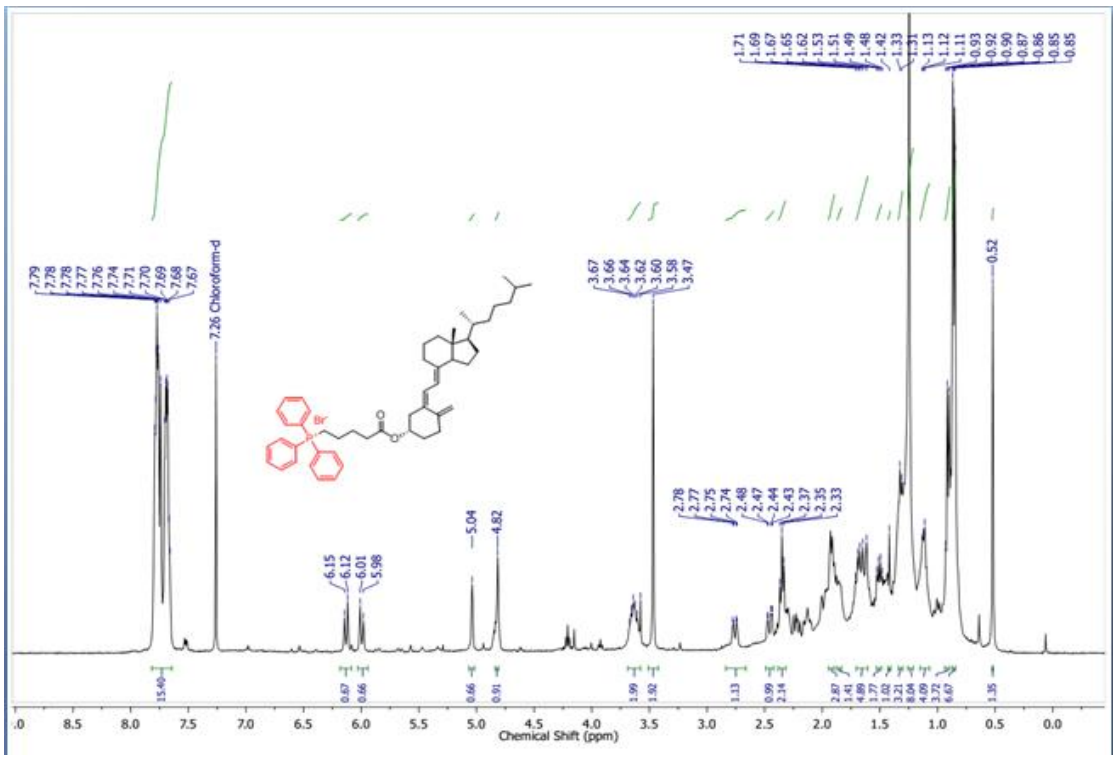

^{13}C NMR (100 MHz, $CDCl_3$) (18)

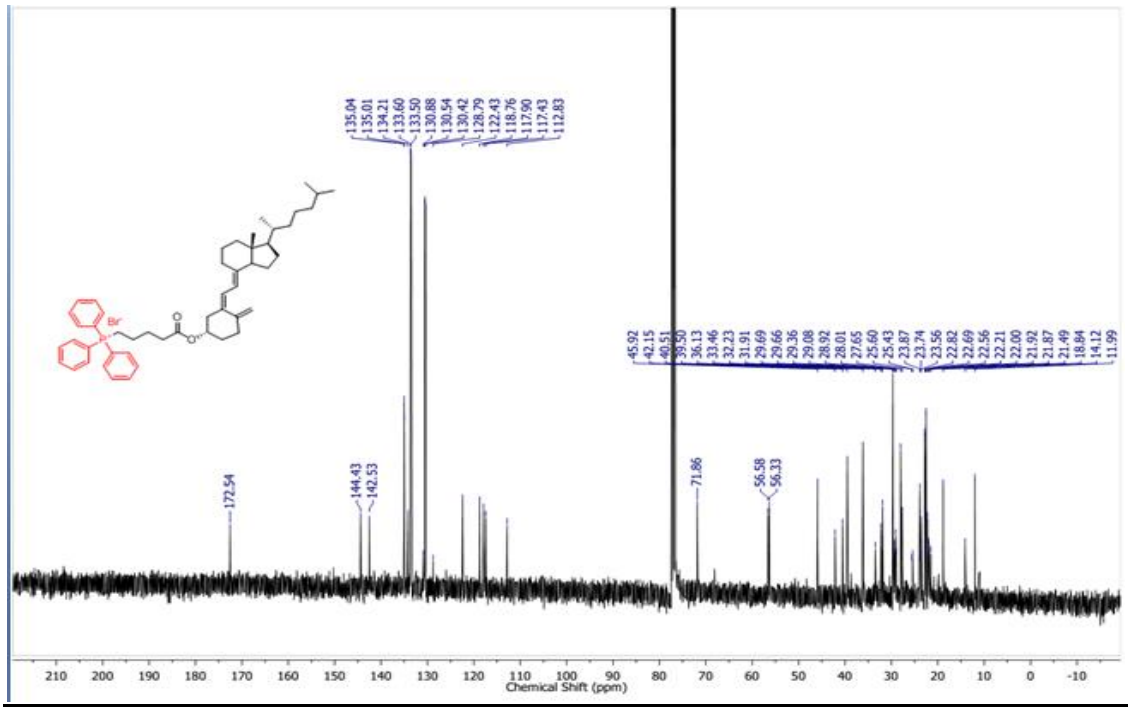

^{31}P NMR ($CDCl_3$) (18)

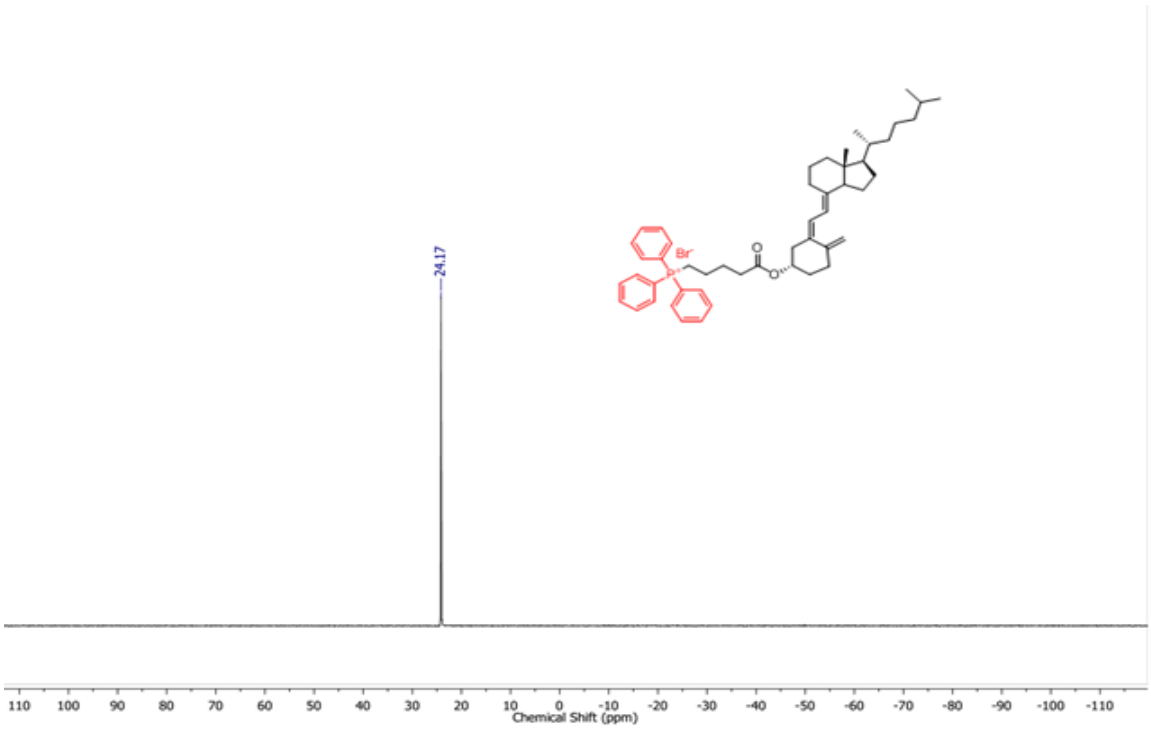

MALDI-TOF Spectrometry (18)